A SUMO-targeted ubiquitin ligase is involved in the degradation of the nuclear pool of the SUMO E3 ligase Siz1

Jason W. Westerbeck*,†, Nagesh Pasupala*, Mark Guillotte, Eva Szymanski, Brooke C. Matson, Cecilia Esteban, and Oliver Kerscher
Biology Department, The College of William & Mary, Williamsburg, VA 23187

ABSTRACT **The Slx5/Slx8 heterodimer constitutes a SUMO-targeted ubiquitin ligase (STUbL) with an important role in SUMO-targeted degradation and SUMO-dependent signaling. This STUbL relies on SUMO-interacting motifs in Slx5 to aid in substrate targeting and carboxy-terminal RING domains in both Slx5 and Slx8 for substrate ubiquitylation. In budding yeast cells, Slx5 resides in the nucleus, forms distinct foci, and can associate with double-stranded DNA breaks. However, it remains unclear how STUbLs interact with other proteins and their substrates. To examine the targeting and functions of the Slx5/Slx8 STUbL, we constructed and analyzed truncations of the Slx5 protein. Our structure–function analysis reveals a domain of Slx5 involved in nuclear localization and in the interaction with Slx5, SUMO, Slx8, and a novel interactor, the SUMO E3 ligase Siz1. We further analyzed the functional interaction of Slx5 and Siz1 in vitro and in vivo. We found that a recombinant Siz1 fragment is an in vitro ubiquitylation target of the Slx5/Slx8 STUbL. Furthermore, *slx5Δ* cells accumulate phosphorylated and sumoylated adducts of Siz1 in vivo. Specifically, we show that Siz1 can be ubiquitylated in vivo and is degraded in an Slx5-dependent manner when its nuclear egress is prevented in mitosis. In conclusion, our data provide a first look into the STUbL-mediated regulation of a SUMO E3 ligase.**

Monitoring Editor
Orna Cohen-Fix
National Institutes of Health

Received: May 31, 2013
Revised: Sep 25, 2013
Accepted: Oct 28, 2013

INTRODUCTION

Eukaryotic cells use the addition and removal of posttranslational modifiers (PTMs) to control the cell division cycle. Ubiquitin and SUMO are two small proteinaceous PTMs that modulate protein fate and function. Ubiquitin is best known for its role in the targeted degradation of important cell-cycle regulators, but it also holds many nonproteolytic functions (reviewed by Ulrich and Walden, 2010; Okita and Nakayama, 2012; Yao and Ndoja, 2012). In contrast, SUMO modification does not necessarily lead to degradation of the proteins to which it is attached. Instead, sumoylation modulates the localization, interaction, and activity of target proteins, including those involved in efficient cell cycle progression, DNA replication and repair, transcriptional regulation, and the formation of nuclear bodies, to name just a few (Wang and Dasso, 2009).

All eukaryotic cells carry several copies of the gene encoding ubiquitin, a conserved 76–amino acid protein. Ubiquitin shares only limited sequence identity with other ubiquitin-like proteins (Ubls)—for example, SUMO (18%)—but the overall "ubiquitin fold" is structurally conserved. Mammalian cells encode three different SUMO isoforms—SUMO1, 2, and 3—whereas budding yeast cells express only one—Smt3—hereafter referred to as yeast SUMO. After translation, both ubiquitin and SUMO precursors are made conjugation competent by processing through ubiquitin- and SUMO-specific proteases, respectively. This processing exposes a carboxy-terminal diglycine motif that is subsequently linked to a lysine side chain of a target protein. The ATP-dependent process of substrate selection and linkage is mechanistically conserved between Ubls. Generally, ubiquitylation and sumoylation of proteins depend on the stepwise

This article was published online ahead of print in MBoC in Press (http://www.molbiolcell.org/cgi/doi/10.1091/mbc.E13-05-0291) on November 6, 2013.

*These authors are joint first authors.

†Present address: Biochemistry, Cellular and Molecular Biology Graduate Program, Johns Hopkins School of Medicine, 720 Rutland Ave., Baltimore, MD 21205.

Address correspondence to: Oliver Kerscher (opkers@wm.edu).

Abbreviations used: NLS, nuclear localization signal; SIM, SUMO-interacting motif; STUbL, SUMO-targeted ubiquitin ligase; SUMO, small ubiquitin-like modifier.

activity of a dedicated cascade of Ubl-specific E1 (activating), E2 (conjugating), and E3 (ligating) enzymes (reviewed by Kerscher *et al.*, 2006). To ensure that the correct protein is modified with ubiquitin, ubiquitin E3 ligases recognize individual substrate proteins (reviewed in Deshaies and Joazeiro, 2009). For the majority of sumoylation events, a consensus motif ψKXE/D (ψ being a large hydrophobic amino acid and X any residue) in the target protein appears sufficient for sumoylation via the E2 conjugating enzyme Ubc9 (Sampson *et al.*, 2001). However, in the absence of sumoylation motifs or to enhance sumoylation on specific proteins, SUMO E3s are required. These include Siz1, Siz2, Mms21, and Zip3 in yeast (Johnson and Gupta, 2001; Zhao and Blobel, 2005; Cheng *et al.*, 2006; Takahashi *et al.*, 2006).

Siz1 and Siz2 account for the majority of E3-mediated sumoylation in yeast. These E3 ligases have some overlapping substrates, whereas others are unique (Reindle *et al.*, 2006). For example, the bud neck–localized septin proteins Cdc3, Cdc11, and Shs1 depend solely on Siz1 for their sumoylation (Johnson and Gupta, 2001; Takahashi *et al.*, 2001a,b). Sumoylation of these septins requires that Siz1 be exported from the nucleus in mitosis, via the karyopherin Msn5, to associate with septins at the bud neck of dividing cells. Msn5 is known to transport phosphorylated cargoes, and the phosphorylation of Siz1, via an unknown kinase, may facilitate its export from the nucleus (Takahashi and Kikuchi, 2005; Takahashi *et al.*, 2008; Makhnevych *et al.*, 2007). In *msn5Δ* cells Siz1 is not exported from the nucleus and septins remain unsumoylated (Makhnevych *et al.*, 2007).

Both ubiquitin and SUMO can form chains on the targets they modify. Ubiquitin has seven lysines, and at least five of these (K6, K11, K29, K48, K63) can serve as conjugation sites for additional ubiquitin molecules (Wickliffe *et al.*, 2009). In contrast, all SUMO variants, except SUMO1, form chains through lysines in their amino terminus. Yeast SUMO has three lysines (K11, K15, and K19), all centered on sumoylation consensus sites, that are required for SUMO-chain formation (Bylebyl *et al.*, 2003; Ulrich, 2008). SUMO chains accumulate due to heat shock, osmotic stress, and replicative stress (Vertegaal, 2010). As detailed later, the exact role of SUMO chains in the cellular stress response is not entirely clear. However, SUMO chains can also become ubiquitylated via SUMO-targeted ubiquitin ligases (STUbLs), and these branched Ubl structures may play an important role in protein degradation and signaling (Guzzo *et al.*, 2012; Guzzo and Matunis, 2013; Nie *et al.*, 2012).

STUbLs, first functionally identified in yeasts, have given credence to a proteolytic role of SUMO. STUbLs are ubiquitin E3 ligases that can specifically target and bind SUMO chains or proteins modified with SUMO chains and facilitate their ubiquitylation, although recent evidence suggests that STUbLs may not always require SUMO or SUMO chains to interact with their substrates (Xie *et al.*, 2010). Members of this unusual family of ubiquitin ligases are exquisitely conserved and have been identified in yeasts, flies, frogs, fish, mice, and humans (reviewed by Prudden *et al.*, 2007; Geoffroy and Hay, 2009; Praefcke *et al.*, 2012). There are four STUbL proteins (Slx5, Slx8, Ris1, Rad18) in the budding yeast *Saccharomyces cerevisiae*, three in fission yeast *Schizosaccharomyces pombe* (Rfp1, Rfp2, and Slx8), and at least one in multicellular eukaryotes, including humans (RNF4; Wang *et al.*, 2006; Sun *et al.*, 2007; Uzunova *et al.*, 2007; Xie *et al.*, 2007; Tatham *et al.*, 2008; Mukhopadhyay *et al.*, 2010; Parker and Ulrich, 2012). Budding yeast Slx5 and Slx8 form a complex that plays an important role in the DNA damage response, genome maintenance, and proteasome-mediated degradation of specific transcriptional regulators. Included in a growing list of experimentally confirmed ubiquitylation targets of Slx5/Slx8 are the transcriptional regulators Mot1 and Matalpha2 (in vivo), the homologous recombination protein Rad52 (in vitro), and sumoylated Nfi1/Siz2 (in vitro; Zhang *et al.*, 2006; Nagai *et al.*, 2008; Cook *et al.*, 2009; Wang and Prelich, 2009; Xie *et al.*, 2010; Garza and Pillus, 2013). In contrast, Ris1 has been proposed to target cytosolic proteins, including sumoylated Pac1, a microtubule-associated protein (Alonso *et al.*, 2012). Rad18, a SIM-containing ubiquitin ligase that is stimulated by sumoylation of its substrate, the sliding clamp protein PCNA, is likely the newest member of a growing family of STUbLs (Parker and Ulrich, 2012). Apart from specific protein substrates, among the most important targets of STUbLs may be SUMO chains. This is illustrated by the observation that STUbL mutants accumulate high–molecular weight SUMO chains (Uzunova *et al.*, 2007; Xie *et al.*, 2007). However, our mechanistic understanding of SUMO chains is limited, and whether these polymers are beneficial or detrimental to cellular processes may depend on several factors, including growth conditions and genetic background (Uzunova *et al.*, 2007; Mullen *et al.*, 2011; Tan *et al.*, 2013). In general, there is also clear evidence that the accumulation of SUMO conjugates in SUMO protease mutants is linked to vegetative growth, cell cycle progression, and other defects (Li and Hochstrasser, 1999, 2000). Of note, Slx5 was identified as a high-copy suppressor of a temperature-sensitive SUMO protease mutant, *ulp1ts* (Xie *et al.*, 2007).

STUbLs use SIMs to interact noncovalently with SUMO, SUMO chains, and sumoylated substrate proteins. A consensus SIM sequence consists of a hydrophobic core (V/I-X-V/I-V/I) that is often juxtaposed with a stretch of acidic and/or phosphorylated amino acids (Kerscher, 2007). Slx5 is the targeting subunit of the Slx5/Slx8 STUbL and contains at least four SIMs, but only two are essential for the interaction with SUMO and the formation of nuclear Slx5 foci (Xie *et al.*, 2007, 2010; Cook *et al.*, 2009). Multiple SIMs in Slx5 are believed to increase the affinity of Slx5/Slx8 for SUMO chains or polysumoylated proteins. SIMs are not limited to STUbLs, and proteins that otherwise lack affinity for each other may use SUMO to interact through SIMs. This can be useful for subcellular targeting and the formation of large protein complexes—for example, during the biogenesis of PML bodies (Lin *et al.*, 2006; Shen *et al.*, 2006). In addition, some proteins contain both SIMs and ubiquitin-interacting motifs, and it is believed that these proteins may be able to interact with hybrid SUMO–ubiquitin chains formed by STUbLs. For example, hybrid SUMO–ubiquitin chains formed by Slx5/Slx8 and RNF4 are recognized by yeast Ufd1 (the substrate-recruiting cofactor of the Cdc48p-Npl4p-Ufd1p complex) and mammalian Rap80 (a ubiquitin-interacting motif containing protein with a role in the DNA damage response), respectively. Thus hybrid SUMO–ubiquitin chains serve as "coded keys" representing a SUMO-dependent signal that helps orchestrate DNA repair functions (Guzzo *et al.*, 2012; Guzzo and Matunis, 2013; Nie *et al.*, 2012).

Here we describe the results of a structure–function analysis of Slx5. In the course of this study we determined that Slx5 interacts with the mitotically regulated SUMO E3 ligase Siz1 in vitro and in vivo. Budding yeast cells exhibit a closed mitosis, and Siz1 is unusual in that it is exported from the intact nucleus at the onset of mitosis to sumoylate septins at the bud neck of dividing cells. Several observations now suggest that Siz1 is a cell cycle–dependent target of the Slx5/Slx8 STUbL. First, Slx5/Slx8 ubiquitylates a Siz1 construct in vitro. Second, we find that *slx5Δ* cells contain increased steady-state levels of phosphorylated and sumoylated Siz1 in vivo. Finally, Siz1 protein that remains in the nucleus after the onset of mitosis is degraded in an Slx5-dependent manner. These data provide a first look into the cell cycle–dependent regulation of SUMO ligase activity via STUbLs.

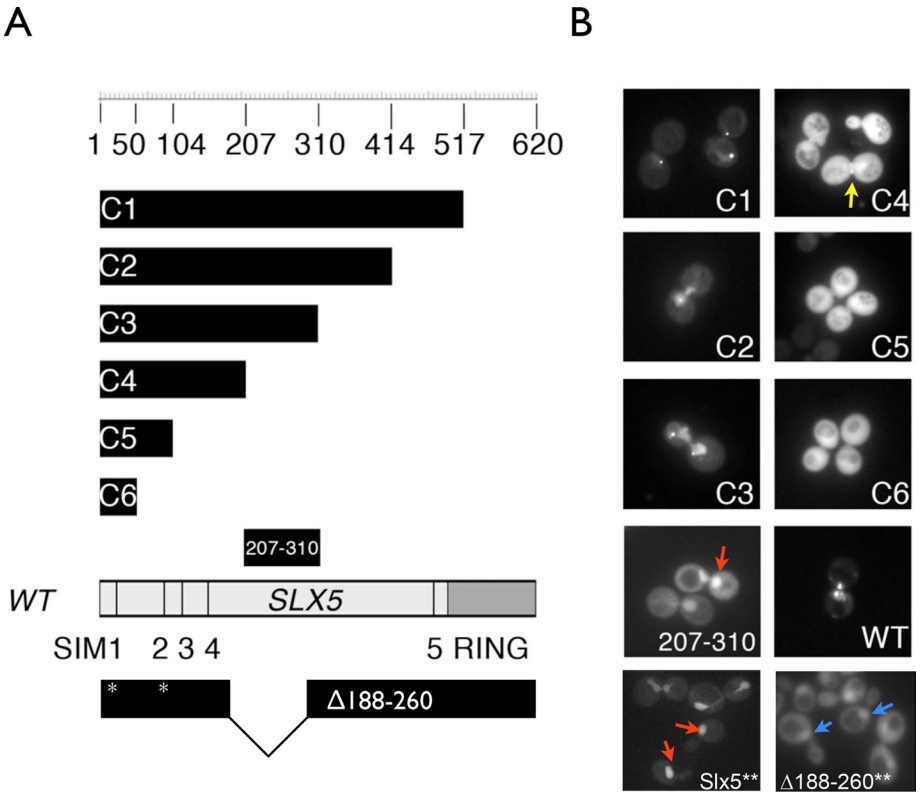

FIGURE 1: Targeting of Slx5 depends on a nuclear-localization domain and SIMs (A) Graphic depiction of six carboxy-terminal truncations (C1–C6) of Slx5. The length of each truncation construct is indicated by the scale above, with full-length Slx5 being 620 amino acids in length. Also indicated are previously identified SIMs and the RING domain (dark gray) of the full-length (WT) Slx5 protein, a small Slx5 domain (207–310) implicated in nuclear localization and dimerization, and a full-length Slx5 deletion construct lacking an arginine-rich region, Δ188–260. Point mutations in Sim1 and 2 are indicated as asterisks. (B) Subcellular localization of GFP-tagged Slx5 truncations (C1–C6) indicated in A. Plasmids expressing GFP-tagged C1–C6 constructs and the Slx5 domain (207–310) were transformed into yeast cells to determine their subcellular localization in comparison to full-length WT Slx5-GFP. Notice nuclear Slx5 foci present in C1 (foci 32 ± 7.3%, $n = 352$), C2 (foci 42.5 ± 3.72%, $n = 271$), and C3 (foci 23 ± 10.5%, $n = 232$). Constructs C4–C6 are distributed throughout the cells, with an additional enrichment of C4 at the bud neck (yellow arrow) of dividing cells (bud neck localization 11.5 ± 1.29%, $n = 374$). GFP-tagged Slx5(207–310) is enriched in the nucleus (red arrows), suggesting that this domain is important for nuclear localization of Slx5. Reciprocally, an overlapping construct, Slx5(Δ188–260)-GFP, is redistributed between the nucleus and the cytosol. The nuclear Slx5-GFP signal averaged 64.5 ± 4.9% ($n = 85$ nuclei, red arrows, bottom) compared with 56 ± 2.3% ($n = 84$ nuclei, blue arrows) in the Slx5(Δ188-260)-GFP mutant (Kruskal–Wallis test, 109.3; $df = 1$; $p < 0.001$). Note that both constructs in the bottom also contain point mutations in Sim1 and Sim2 (indicated by asterisks) to ensure that the localization was unbiased of association with SUMO and sumoylated proteins in the nucleus and the cytosol. Furthermore, the localization of both constructs in the bottom was evaluated in an *slx5/slx8* double mutant to prevent association with endogenous Slx5 and Slx8. *n*, number of log-phase cells imaged and analyzed ± SD.

RESULTS

Targeting of Slx5 depends on a nuclear-localization domain and SIMs

Slx5 is the targeting subunit of the heterodimeric Slx5/Slx8 STUbL complex in budding yeast. The Slx5 protein contains at least four SIMs (amino acids 24–158) and a carboxy-terminal RING domain (amino acids 490–620; Figure 1A; Mullen *et al.*, 2001; Uzunova *et al.*, 2007; Xie *et al.*, 2007, 2010; Cook *et al.*, 2009). We previously reported that SIMs in Slx5 are involved in the formation of nuclear foci, whereas the RING domain is required for substrate ubiquitylation by the Slx5/Slx8 heterodimer (Xie *et al.*, 2007; Cook *et al.*, 2009).

Considering the important role of STUbLs in DNA repair and genome maintenance, we asked whether particular domains of Slx5 are required for nuclear localization. Therefore we determined the localization of six carboxy-terminal (C1–C6) Slx5 truncations in yeast (Figure 1A). These Slx5 truncations differed by ~100 amino acids (aa) in length, with one exception. The Slx5 construct C6 was 50 aa in length and contained only SIM1 of Slx5 (Figure 1A). All green fluorescent protein (GFP)–tagged Slx5 truncations and the full-length Slx5-GFP control (Cook *et al.*, 2009) were expressed under control of the native Slx5 promoter from low-copy plasmids. Representative images of live yeast cells expressing GFP-tagged Slx5 truncations were recorded at early log phase (Figure 1B). Image analysis of our Slx5-GFP constructs revealed that the absence of the Slx5 RING domain (aa 490–620) and SIM5 (476–479) does not grossly affect nuclear localization and formation of nuclear foci (constructs C1 and C2; see Figure 1 legend for incidence of foci). Of interest, a truncation consisting only of the amino-terminal half of Slx5 (C3: 1–310) was still enriched in the nucleus. This nuclear localization was abruptly altered in a slightly shorter Slx5-GFP truncation (C4: Slx5-GFP(1–207)). Slx5-GFP(1–207) appeared to reside both in the cytoplasm and in the nucleus and lacked distinct foci. It is unlikely that the Slx5-GFP(1–207) fusion protein simply leaked from the nucleus because this GFP-tagged Slx5 truncation is larger (57 kDa) than the defined molecular weight for passive nuclear diffusion (Shulga *et al.*, 2000). As expected, constructs that were even smaller than Slx5(1–207)-GFP—C5(1–104) and C6(1–50)—also failed to be enriched in the nucleus.

We further investigated the functional relevance of the Slx5(207–310) domain. Fusion of Slx5(207–310) to GFP revealed that this domain, when expressed in wild-type yeast cells, is involved in nuclear localization. Slx5(207–310)-GFP shows a diffuse nuclear enrichment with some residual cytosolic staining (Figure 1B, 207–310). We were unable to identify a specific NLS in this domain but noticed that the overlapping region from amino acid 188 to 260 was enriched in arginine residues. Therefore we generated an Slx5(Δ188–260)-GFP construct and found that its nuclear localization was reduced, with a concomitant redistribution to the cytosol (Figure 1B). Image analysis revealed a significant reduction of nuclear localization (Kruskal–Wallis test, 109.3; $df = 1$; $p < 0.001$) for the Slx5(Δ188–260)-GFP mutant. However, because nuclear localization of the deletion mutant is not completely abolished, we conclude that additional determinants of nuclear localization may reside in the carboxy terminus of Slx5.

A truncation of Slx5 is enriched at the bud neck of dividing cells

Careful analysis of the carboxy-terminal truncations of Slx5 revealed that Slx5-GFP(1–207) not only accumulated in the cytoplasm but also was visibly enriched at the bud neck of dividing cells (11.5 ± 1.29%, $n = 374$; Figure 1B). We reasoned that this localization was due to the SIM-mediated association of Slx5(1–207)-GFP with sumoylated septins at the bud neck. Septins, including Cdc3, Cdc10, Cdc11, Cdc12, and Shs1, form a filamentous ring structure at the bud neck between mother and daughter cell of dividing yeast (Douglas *et al.*, 2005; Cao *et al.*, 2009). SUMO modification of Cdc3, Cdc11, and Shs1 in mitosis plays an important role in septin ring dynamics (Johnson and Blobel, 1999) but may also serve to recruit SIM-containing and SUMO-binding proteins in mitosis (Kusch *et al.*, 2002; Elmore *et al.*, 2011).

To test whether Slx5(1–207) colocalized with individual septins, we chromosomally tagged *CDC3* with the gene encoding the yellow fluorescent protein (YFP; YOK1325). This *CDC3-YFP* strain was then transformed with a plasmid encoding Slx5(1–207) fused to the gene encoding the cyan fluorescent protein (CFP; strain YOK1364). Live imaging of G2/M-arrested cells revealed that both Cdc3-YFP and Slx5(1–207)-CFP fusion proteins were expressed and colocalized to septin rings in the majority (~80%) of large-budded cells (Figure 2A). In logarithmically growing cells colocalization of Slx5(1–207)-CFP and Cdc3-YFP to one or two septin rings was observed (~20%). However, as expected, the colocalization was limited to large-budded cells in mitosis.

Next we tested our hypothesis that the localization of Slx5(1–207)-GFP to the septin ring was dependent on SUMO. We examined the ability of Slx5(1–207) with SIM1/2 mutations (25-AAA-27 and 93-ATAA-96) to bind to septins. We previously showed that SIM1 and SIM2 play a critical role in the formation of Slx5 nuclear foci and SUMO binding (Xie *et al.*, 2007; Cook *et al.* 2009). The Slx5(1-207) SIM1/2 mutant and a control plasmid with intact SIMs were transformed into a wild-type strain, and G2/M-arrested cells were examined. The Slx5(1–207) construct was localized throughout the cell but was also visually enriched at the bud neck of 65% of G2/M-arrested cells (Figure 2B, top left). Of note, the enrichment of the Slx5(1–207) SIM1/2 mutant at septins was barely visible, and only a few cells displayed residual staining at the bud neck (Figure 2B, top right). Next we expressed Slx5(1–207)-GFP in a strain that is unable to form polySUMO chains (smt3-R11,15,19; Bylebyl *et al.*, 2003). Here we found that Slx5(1–207) septin localization was reduced to ~27% but not eliminated in *smt3(R11,15,19)* cells (Figure 2B, bottom left).

Finally, we also tested a deletion of the SUMO E3 ligase gene *SIZ1*, which is required for the sumoylation of bud neck–localized septins in mitosis (Johnson and Blobel, 1999). Consistent with the foregoing data, Slx5(1–207)-GFP localization to septins was greatly reduced or absent in *siz1Δ* cells (Figure 2B, bottom right). In summary, these data suggest that the bud neck localization of the cytosolic Slx5(1–207) truncation depends on both the cell cycle–specific sumoylation of septins and the SIMs in Slx5. However, we cannot exclude the possibility that Siz1 recruits this construct to the bud neck. Even though we found no evidence that septins are physiological targets of this STUbL subunit, our observations provide a visual in vivo assay for SUMO-dependent targeting of Slx5 to a highly sumoylated target, the septins (Elmore *et al.*, 2011).

The STUbL subunit Slx5 has distinct and separate domains for interaction with Slx8, Slx5, and SUMO

The results obtained in our localization studies (Figure 1B) raised the possibility that individual domains of Slx5 may functionally interact

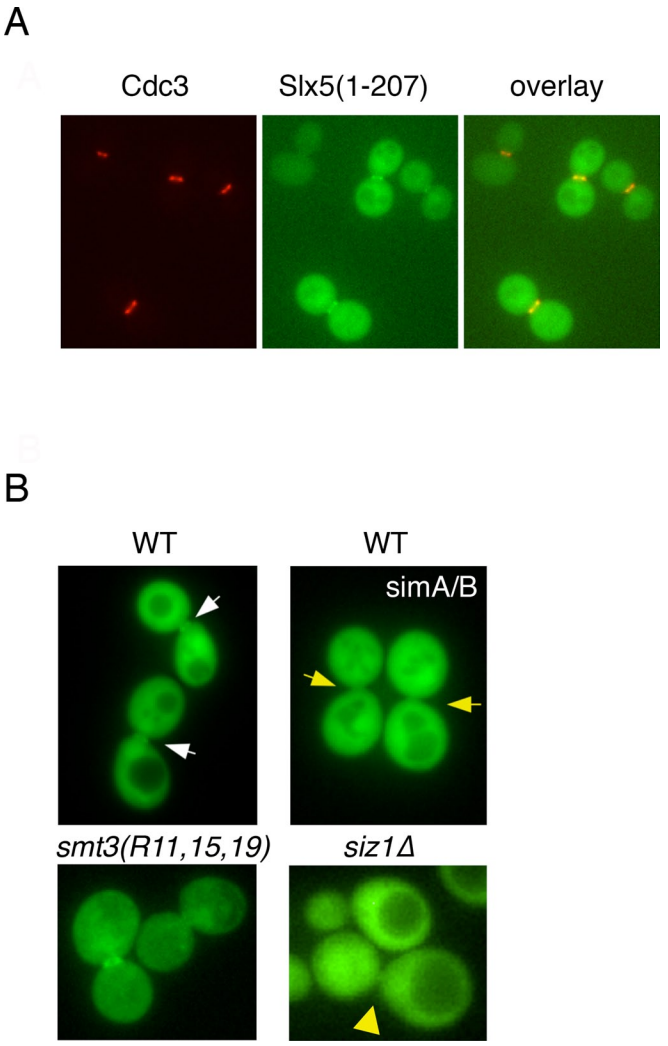

FIGURE 2: A Slx5 truncation containing four SIMs but lacking the potential nuclear localization domain (207–310) is enriched at the septin ring of G2/M-arrested cells. (A) Cells expressing the YFP-tagged septin protein Cdc3-YFP (YOK1325) were transformed with SLX5(1-207)-CFP (compare construct C4; BOK 507) and then arrested in G2/M before microscopic analysis in live cells. Slx5(1-207)-CFP was present diffusely throughout the cells but was visibly enriched at the bud neck of G2/M-arrested cells (pseudocolored in green), where it colocalized with Cdc3-YFP at the septin ring (pseudocolored in red). Colocalization was observed in ~80% of cells showing expression of both constructs. (B) The bud neck localization of SLX5(1–207) depends on SIMs and the SUMO ligase Siz1. SLX5(1–207)-GFP (BOK505) and a mutant lacking SIM1 and 2 (1–207(Δsim1/2)) were transformed into yeast cells to determine the requirement for bud neck localization of each construct in G2/M-arrested cells (top left and right). Slx5(1-207)-GFP septin enriched at the bud neck of G2/M-arrested cells was observed in 65 ± 15% of WT cells ($n = 162$, white arrows). In contrast, septin localization of Slx5(1–207(Δsim1/2)) was greatly reduced or absent ($n = 108$, yellow arrows). The localization of Slx5(1–207)-GFP was then analyzed in a strain expressing a mutant SUMO protein that fails to form chains (bottom left, *smt3(R11,15,19)* or strains deleted for the SUMO ligase Siz1, which sumoylates septins (bottom right, *siz1Δ*). Note that bud neck localization was still observed in 27.4 ± 14.9% of *smt3(R11,15,19)* cells ($n = 338$) but not in the *siz1Δ* mutant (yellow arrowhead). *n*, number of G2/M-arrested cells imaged and analyzed.

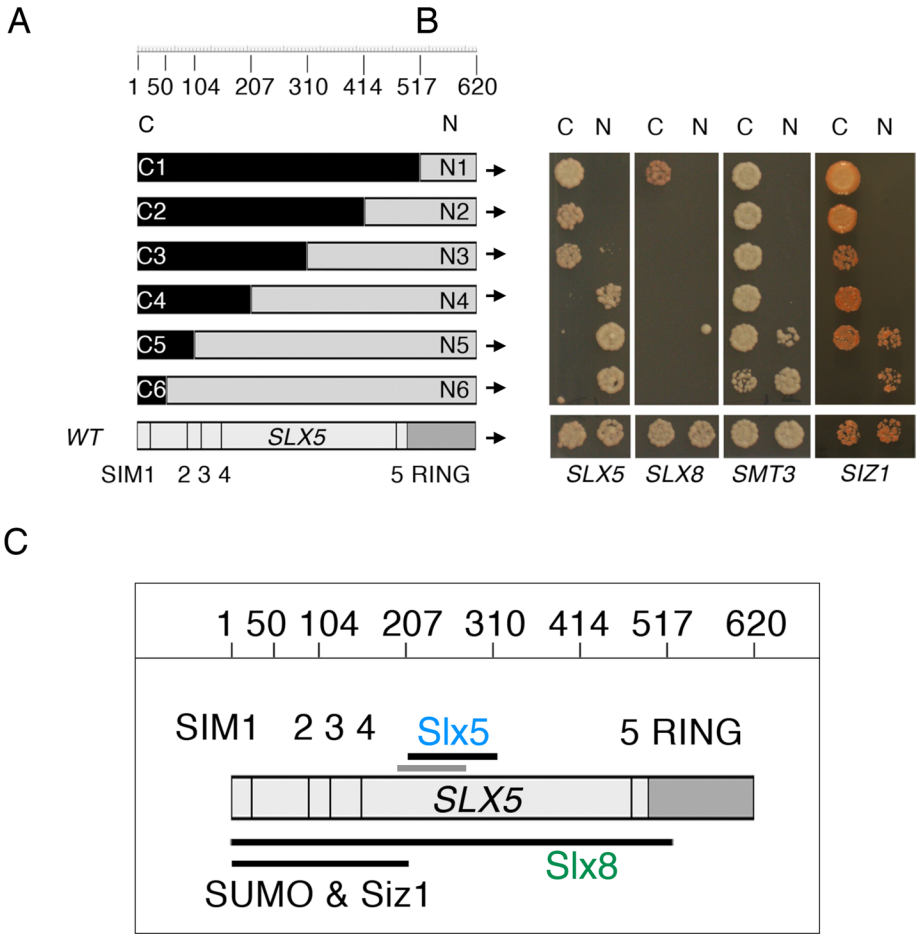

FIGURE 3: Slx5 uses distinct domains to interact with Slx8, Slx5, yeast SUMO (Smt3), and Siz1. (A) Graphic depiction of six carboxy-terminal deletions (C1–C6) and six amino-terminal deletions (N1–N6) of Slx5. The length of each truncation construct is indicated by the scale above, with full-length Slx5 being 620 amino acids in length. Also indicated are previously identified SIMs and the RING domain (dark gray) of the full-length (WT) Slx5 protein. (B) Analysis of two-hybrid interaction of WT Slx5 and various Slx5 truncations (C & N). Duplicate spots of yeast cell colony patches indicate two-hybrid interactions of Slx5 with full-length Slx5, Slx8, Smt3, and Siz1 (bottom). Interactions of Slx5, Slx8, Smt3, and Siz1 with individual Slx5 truncations (amino-terminal, N1–N6; carboxy-terminal, C1–C6) correspond to the Slx5 truncations in A (see arrows). Refer to *Materials and Methods* for details of the two-hybrid analysis. Note that the domain encompassing amino acids 207–310 of Slx5 is required for interaction with full-length Slx5 and that the interaction pattern of Slx5 with SUMO (Smt3) mirrors that with Siz1. (C) Graphic depiction of Slx5 interaction derived from our structure–function analysis in Figures 1 and 2 and this figure. Depicted are Slx5 amino acids 1–620 (increments indicate our constructs), with SIM1–5 and the RING domain, an arginine-rich domain that may be involved in nuclear localization that overlaps the Slx5 interaction domain and is marked with a gray bar.

with different proteins such as sumoylated substrates, other STUbL subunits, or nuclear transport factors.

To test this hypothesis, we initially focused on the interaction of Slx5 with two known interactors, SUMO and Slx8 (Ii *et al.*, 2007; Xie *et al.*, 2007; Mullen and Brill, 2008). Specifically, we delineated the interaction domains of Slx5 using a collection of six amino-terminal (N1–N6) and six carboxy-terminal Slx5 bait truncations (C1–C6; Figure 3A). Full-length or truncated Slx5 bait constructs (Gal4-BD fusions) were cotransformed with the appropriate prey constructs (Gal4-AD fusion of Slx8 or SUMO) into a two-hybrid reporter strain (AH109). Bait/prey interactions were scored as growth of double transformants on growth media lacking adenine and/or histidine (Figure 3B). Our data confirmed that full-length Slx5 interacts with SUMO and Slx8 (Figure 3B, bottom). Furthermore, we unexpectedly found that a full-length Slx5 bait can also interact with other Slx5 prey proteins, raising the possibility that this STUbL subunit, similar to its human orthologue RNF4, may homodimerize (Liew *et al.*, 2010).

Analysis of the Slx5 bait truncations reveals that at least one SIM (SIM1: 24VILI27) is required for interaction with yeast SUMO (Smt3; Figure 3: C6 with SUMO). In contrast, the interaction of Slx5 bait with other Slx5 prey proteins was independent of SIM1, 2, 3, and 4 and dependent on a novel domain between amino acids 207 and 310 (Figure 3: N4 and C3 with *SLX5*). Of interest, Slx5(207–310) overlapped with the domain involved in nuclear localization of Slx5 (Figure 1B, red arrow). One possible explanation for this finding is that homodimerization is required for nuclear import or nuclear retention of Slx5. Several examples of proteins that require dimerization for nuclear import exist (Fryrear *et al.*, 2009; Hayes *et al.*, 2009). However, dimerization of Slx5 is a possibility that requires further investigation.

The interaction of Slx5 with Slx8 was more complex. One *SLX5* truncation (C1), retaining only two cysteine residues (Cys-494 and Cys-497) of the RING domain, showed a reproducible interaction with Slx8. Surprisingly, none of the Slx5 amino-terminal deletions (N1–N6) scored positive in our interaction assay with Slx8. This suggests that the amino terminus but not the entire RING domain of Slx5 is required for interaction with Slx8. To further investigate how Slx5 interacts with Slx8, we used a full-length Slx5 bait construct lacking both SIM1 and SIM2 (Slx5(Δsim1/2); Xie *et al.*, 2007). Full-length Slx8 prey and full-length Slx5(Δsim1/2) bait were cotransformed into the two-hybrid assay strain. As a control, both constructs were also tested against *SMT3* and *SLX5* constructs. In accordance with the foregoing data, the Slx5(Δsim1/2) mutant interacted strongly with Slx5, failed to interact with Smt3, and was greatly reduced in its interaction with Slx8 (Supplemental Figure S1). Therefore both SIMs and the RING domain of Slx5 may be important for the interaction with Slx8. In summary, our two-hybrid fine-structure mapping defines four distinct Slx5 domains required for interaction with Smt3 (aa 1–207), Slx5 (aa 207–310), and Slx8 (aa 1–50 and 490–620).

The STUbL subunit Slx5 forms a complex with the SUMO ligase Siz1

Because Slx5(1–207) localized to septin rings in a SUMO-targeting assay, we decided to test its interaction with potential sumoylated substrate proteins at the bud neck. Despite its enrichment at the septin ring, Slx5(1–207) failed to interact with the septins Cdc3 and Cdc11 (unpublished data). However, Slx5 interacted in a two-hybrid assay with a known septin-interacting protein, the SUMO E3 ligase Siz1 (Figure 3B, bottom right). Siz1 resides in the nucleus but

becomes enriched on the septin ring during the G2/M phase of the cell cycle, presumably to sumoylate septins. Accordingly, in the absence of Siz1, septins, including Cdc3 and Cdc11, fail to be sumoylated (Johnson and Gupta, 2001).

We decided to investigate which domain of Slx5 was required for the interaction with Siz1. Using our panel of 12 Slx5 two-hybrid baits, we found that interaction with Siz1 requires at least two SIMs (SIM1 and 2) in Slx5 (Figure 3B, construct C5). The observed interaction closely mirrors the pattern we observed for interaction between our Slx5 bait constructs and SUMO. This suggests that the interaction of Slx5 with Siz1 may depend on SUMO and possibly sumoylation of Siz1. Indeed, when we tested the interaction of Siz1 with the Slx5(Δsim1/2) or a Siz1-RING mutant (Siz1$^{(C377S\ H379A)}$), we no longer observed the interaction (Supplemental Figure S1).

To confirm our finding of the Slx5–Siz1 interaction, we tested whether both proteins could interact in vitro and in vivo. First we probed the ability of recombinant Slx5 and Slx8 to interact with a purified truncation of Siz1 (Siz1(Δ440)). Siz1(Δ440) lacks the carboxy-terminal 439 amino acids but retains its SUMO ligase activity and can be stably expressed in bacterial and yeast cells (Takahashi and Kikuchi, 2005). To accomplish this task, we mixed bacterial protein extracts containing overexpressed maltose-binding protein (MBP) fusions of Slx5 or Slx8 (Xie *et al.*, 2007) with bacterial extracts containing overexpressed, T7-tagged Siz1(Δ440). Extracts were then passed over amylose affinity resins. We observed that Siz1(Δ440) bound to the amylose affinity resins only when Slx5-MBP or Slx8-MBP was also bound (Figure 4A, lanes 1 and 2). This suggests that recombinant Siz1(Δ440) can interact with both Slx5 and Slx8 in vitro.

Second, we constructed a yeast strain in which glutathione *S*-transferase (GST)–tagged Slx5 and V5-tagged Siz1(Δ440) were both expressed from plasmids under control of the strong inducible Gal promoter. From lysates of this strain, Slx5-GST was affinity purified on glutathione agarose, and copurifying Siz1(Δ440)-V5 was detected after immunoblotting with an anti-V5 antibody (Figure 4B, lanes 5 and 7). In contrast, Siz1(Δ440) expressed in the absence of Slx5-GST did not bind to glutathione agarose (Figure 4B, compare lanes 3 [flowthrough] and 6 [elution]). In summary, we conclude that the SUMO ligase Siz1 can form a complex with the STUbL-targeting subunit Slx5 in yeast cells.

Siz1 is an in vitro and in vivo ubiquitylation substrate of Slx5/Slx8

The evidence presented here suggests that Siz1 forms a complex with Slx5 in living cells. Therefore we tested Siz1 as a candidate substrate for the Slx5/Slx8 STUbL. We purified the Siz1(Δ440) truncation and combined it with recombinant Slx5 and Slx8 in an in vitro ubiquitylation reaction (see *Materials and Methods*). In this assay we found Siz1(Δ440) to be ubiquitylated in an ATP-, E2-, and E3 (Slx5/Slx8)-dependent manner (Figure 5A). Addition of an amino-terminal SUMO moiety to Siz1(Δ440), forming SUMO-Siz1(Δ440), did not dramatically stimulate the ubiquitylation of this fusion protein (unpublished data). This is in accordance with the previous finding that, at least in vitro, SUMO modification is not an absolute requirement for the specific ubiquitylation by Slx5/Slx8 (Xie *et al.*, 2007, 2010). Another interesting observation is that Siz1 is robustly ubiquitylated by Slx5/Slx8, but only with two or three ubiquitin moieties. One possibility is that more extensive ubiquitylation of Siz1 can take place in vivo.

Consequently, we tested whether Siz1 is also ubiquitylated in vivo. Briefly, we used a ubiquitin-shift assay to compare adducts of yeast-expressed Siz1Δ440, modified either with myc-tagged or

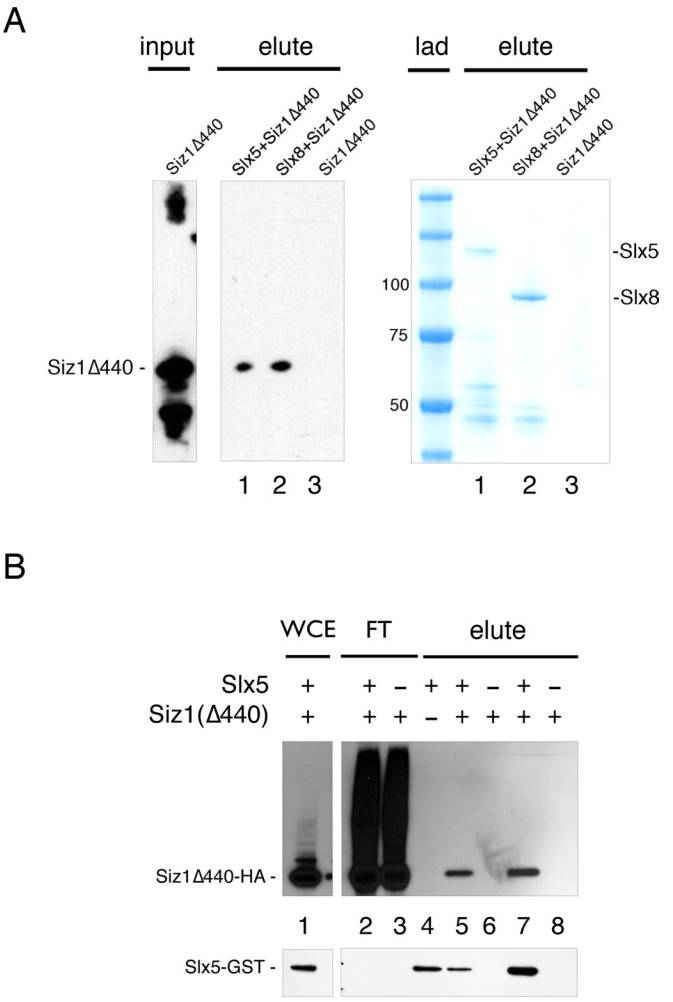

FIGURE 4: The STUbL subunit Slx5 forms a complex with the SUMO ligase Siz1. (A) Slx5 and Slx8 interact with Siz1 in vitro. Recombinant MBP-Slx5, MBP-Slx8, and T7-tagged Siz1(Δ440)-His6 (BOK 500, BOK 501, BOK 758) were produced in bacterial cultures. Then 50 OD units of induced Slx5 and Slx8 cultures were individually combined with 50 OD units of Siz1(Δ440). Siz1(Δ440), 50 OD units, served as a negative control. Whole-cell extracts from the combined or control cultures (Input) were clarified by centrifugation and passed over a column containing amylose resin. After extensive washing, eluates (elute) corresponding to ~1 OD unit of input material were analyzed with an anti-T7 antibody (left). Simply Blue staining (Life Technologies) of a gel with duplicate samples (1–3) reveals the bound recombinant Slx5 (~125 kDa) and Slx8 (~90 kDa) but not the control Siz1(Δ440) protein (~60 kDa) on the amylose resin (right). (B) Slx5 interacts with Siz1 in vivo. We harvested 20 OD units of cells from strains overexpressing GST-Slx5 only (YOK 2507), GST-Slx5 and Siz1(Δ440)-HA (YOK 2509), or Siz1(Δ440)-HA only (YOK 2508) and prepared protein extracts by bead-beating. Clarified extracts were passed over individual glutathione agarose columns, and bound proteins were eluted after extensive washing with 10 mM reduced glutathione (lanes 4–6) or sample buffer (lanes 7 and 8). Also shown are input material (0.3% of total OD harvested) for strain YOK 2509 (lane 1) and flowthrough for strains YOK 2509 and YOK 2508 (lanes 2 and 3). "Elute" loaded corresponds to 0.45% of total OD harvested. Presence or absence of Slx5-GST and Siz1(Δ440)-HA in each sample is indicated as + or –, respectively. All samples were separated by SDS–PAGE, and individual proteins were detected after Western blotting using anti-GST or anti-HA antibodies as indicated. Note that Siz1(Δ440) is only eluted when Slx5-GST is bound to the affinity resin (lanes 5 and 7), indicating an in vivo interaction between the two proteins.

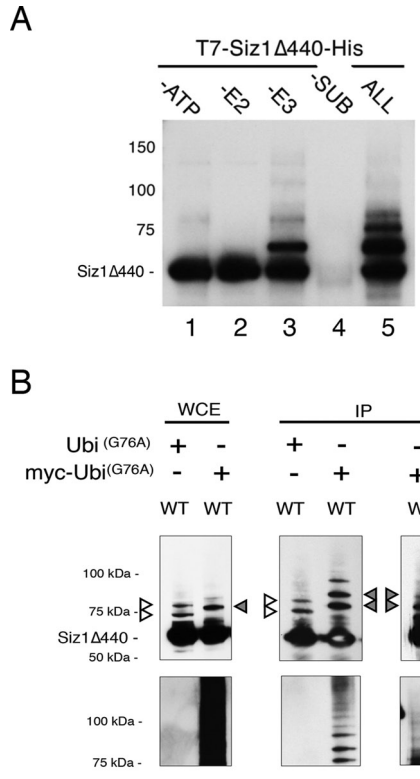

FIGURE 5: Ubiquitylation of Siz1 by Slx5/Slx8 in vitro. In vitro STUbL ubiquitylation reactions, detailed in *Materials and Methods*, were assembled with the recombinant proteins E1 (Uba1), E2 (Ubc4), and E3 (Slx5 and Slx8), ATP, and substrate (SUB, Siz1(Δ440)). As controls, individual components were omitted from the indicated reactions in lanes 1–4 (–ATP, –E2, –E3, –SUB). After incubation, the substrate protein in all reactions was analyzed by immunoblotting with an anti-T7 antibody. Lane 5 contains the complete reaction (ALL) and reveals STUbL-dependent ubiquitylation of Siz1 (Siz1(Δ440)-$(Ub)^n$ (lane 5). Molecular weights in kilodaltons are indicated on the left. (B) Slx5-dependent ubiquitylation of Siz1Δ440 in vivo. Siz1Δ440 was expressed in yeast cells (WT or *slx5Δ*), and a ubiquitin-shift assay was used to compare adducts of Siz1Δ440 modified either with myc-tagged or untagged ubiquitin G76A (+ or –). Siz1Δ440 was detected in whole-cell TCA extracts (WCE) or after immunoprecipitation with anti-V5 agarose (IP). Differentially shifted ubiquitylated adducts of Siz1Δ440 are indicated with white and gray arrows (top). Bottom, Western blots of the same samples probed with an anti-myc antibody to reveal shifted bands that correspond to myc-tagged ubiquitin.

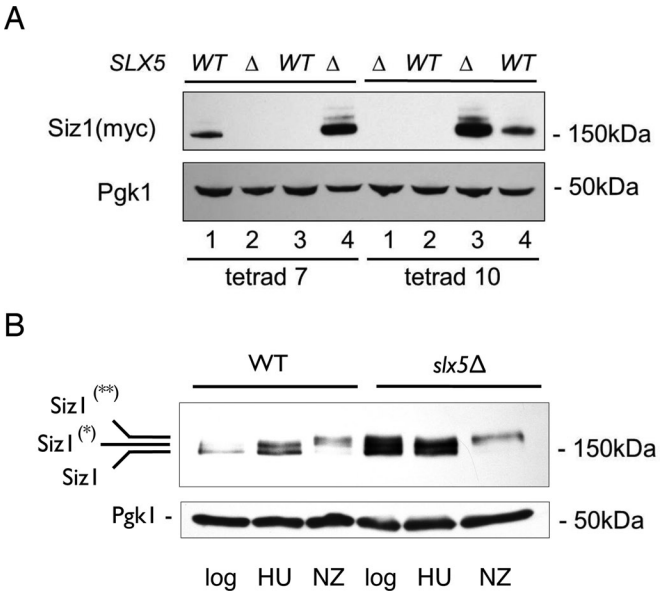

FIGURE 6: Slx5 affects the steady-state level and phosphorylation status of Siz1. (A) Altered steady-state level of Siz1 in *slx5Δ* cells. A heterozygous diploid *SLX5/slx5Δ SIZ1/SIZ1-myc/HIS3* strain was sporulated, and the resulting haploid progeny of two tetrads (tetrad 7 [YOK 2279-2282] and tetrad 10 [YOK 2283-2286]) were genotyped (WT and Δ). Proteins were extracted from the indicated haploid strains to determine the steady-state levels of the myc-tagged Siz1 protein in WT and *slx5Δ* progeny. An anti-myc antibody was used to detect Siz1 on immunoblots of SDS–PAGE–separated proteins. Note the increased steady-state levels and modifications of Siz1 in *slx5Δ* strains (tetrad 7-4 and tetrad 10-3) in comparison to Siz1 levels in WT strains (tetrad 7-1 and tetrad 10-4). Equal protein loading of all extracts was determined using an anti-Pgk1 antibody. (B) Siz1 is differentially phosphorylated under various growth conditions in WT (YOK 2286) vs. *slx5Δ* (YOK 2264) cells. Log, untreated, logarithmically growing cells; HU, hydroxyurea treatment to arrest in S phase; NZ, nocodazole treatment to arrest in G2/M. Endogenous, myc-tagged Siz1 protein in WT and *slx5Δ* cells was detected after immunoblotting of SDS–PAGE–separated proteins using an anti-myc antibody. Single and double asterisks denote differentially phosphorylated forms of Siz1. Equal protein loading of all extracts was determined using an anti-Pgk1 antibody.

untagged ubiquitin G76A ($Ubi^{(G76A)}$). $Ubi^{(G76A)}$ can still be conjugated to proteins but is resistant to deubiquitylation, making it a useful tool for studying potential ubiquitylation targets such as Siz1Δ440 (Hodgins *et al.*, 1992). Whole-cell extracts and immunoprecipitations show differentially shifted Siz1Δ440 adducts, indicating that the protein is ubiquitylated in vivo (Figure 5B, left and middle). These adducts resembled those seen in the in vitro assays. Using the same technique, we also showed that ubiquitylation of Siz1 is dramatically reduced in an *slx5*Δ mutant (Figure 5B, right). Therefore we conclude that the Slx5/Slx8 STUbL can ubiquitylate Siz1Δ440 in vitro and in vivo.

Slx5 affects the steady-state level, phosphorylation, and sumoylation of Siz1 in vivo

Our data are consistent with a role for Slx5 and STUbL-mediated regulation of Siz1. To address the functional relevance of this interaction, we determined the steady-state level of chromosomally expressed Siz1 protein in wild-type (WT) and *slx5Δ* strains. Briefly, an *slx5Δ* strain expressing myc-tagged Siz1 was backcrossed to an isogenic WT strain. As expected, in meiotic progeny that expressed myc-tagged Siz1, the protein was detected as a distinctive band running just below the 150-kDa marker after Western blotting with a myc-specific antibody (Figure 6A, tetrad 7, spores 1 and 4, and tetrad 10, spores 3 and 4). Surprisingly, the steady-state levels of the Siz1 protein in *slx5Δ* strains (Figure 6A, tetrad 7, spore 4, and tetrad 10, spore 3) were markedly enhanced in comparison to the WT (tetrad 7, spore 1, and tetrad 10, spore 4). In addition, increased levels of high–molecular weight adducts of Siz1-myc, consistent with its sumoylation, were visible in the *slx5Δ* strain. Siz1 was previously shown to be autosumoylated in vivo, and these data are consistent with our analysis of in vivo Siz1 sumoylation in a SUMO shift assay and after metal affinity chromatography (Supplemental Figure S2; Takahashi and Kikuchi, 2005).

It is also well established that Siz1 is phosphorylated by an unknown kinase, and, as described earlier, this modification may be linked to its nuclear export before septin sumoylation (Johnson and

Gupta, 2001; Makhnevych *et al.*, 2007). Therefore we also investigated the phosphorylation status of Siz1 in *slx5Δ* and WT cells. First we observed the phosphorylation of Siz1 in both *slx5Δ* cells and WT cells when cells were logarithmically grown, arrested in S phase with hydroxyurea (HU), or arrested in G2/M with nocodazole (Figure 6B). We confirmed the phosphorylation of Siz1 on Phos-tag gels (Wako Pure Chemicals Industries, Osaka, Japan), which further separated phosphorylated and unphosphorylated forms of the protein. In our analysis we found that the levels of both unphosphorylated and two discernible forms of phosphorylated Siz1 were markedly enhanced in *slx5Δ* cells. The effect of *slx5Δ* was less pronounced after HU and nocodazole treatment, with almost complete phosphorylation of Siz1 in nocodazole-arrested *slx5Δ* and WT cells.

PIAS1, an orthologue of Siz1 in mammalian cells, is phosphorylated by casein kinase 2 (Stehmeier and Muller, 2009). However, in our experiments deletion of *CKB1*, the nonessential β regulatory subunit of casein kinase 2 in budding yeast, did not appear to affect the phosphorylation status of Siz1 (unpublished data). In summary, our data reveal that the steady-state levels of both phosphorylated and unphosphorylated Siz1 are increased in *slx5Δ* cells and that cell cycle–dependent phosphorylation of Siz1 may somehow be involved in its regulation.

Slx5 is required to modulate the levels of Siz1 in the nucleus

We devised and tested a model to understand the functional interaction of Slx5 with Siz1 during mitosis. This model takes into account that nuclear export and septin ring localization of Siz1 requires the karyopherin Msn5 and that in an *msn5Δ* mutant Siz1 accumulates in the nucleus, most likely in its phosphorylated form (Johnson and Gupta, 2001; Makhnevych *et al.*, 2007). We reasoned that nuclear retention of Siz1 could make it a substrate of the yeast Slx5/Slx8 STUbL. Therefore we asked what would happen when nuclear egress of the Siz1 protein is prevented in *msn5Δ* cells.

First, we observed GFP-tagged Siz1 in wild-type cells and compared it to *slx5Δ*, *msn5Δ*, and the *msn5Δslx5Δ* double mutant in logarithmically growing and G2/M-arrested cells. Consistent with previous results, Siz1-GFP is a nuclear protein but relocalizes to the septin ring of G2/M-arrested wild-type cells (Figure 7A). We observed a similar localization in *slx5Δ* cells even though septin localization was reduced by ~20%. However, in both the *msn5Δ* and the *msn5Δslx5Δ* mutant, Siz1 was retained in the nucleus and could not be detected at the septin ring. Of note, nuclear Siz1-GFP levels in the *msn5Δslx5Δ strain* were considerably more pronounced than in *msn5Δ* cell. The Siz1-GFP signal in the nucleus of *msn5Δ* cells averaged 60.1 ± 5.9% ($n = 62$ nuclei) compared with 70.6 ± 3.5% ($n = 86$ nuclei) in the *msn5Δslx5Δ strain*. These values represent a significant increase of nuclear enrichment (Kruskal–Wallis test, 81.3; $df = 1$; $p < 0.001$) in the absence of Slx5. This observation is consistent with the accumulation of Siz1 in *slx5Δ* mutants and prompted us to further examine Siz1 levels in these mutants.

To confirm our observation, we performed a cycloheximide chase of Siz1 in mitotically arrested WT and *msn5Δ* cells. Indeed, we found that the half-life of Siz1 was dramatically reduced in the *msn5Δ* strain, with little endogenous Siz1 remaining after 60 min (Figure 7B). In comparison, both phosphorylated and nonphosphorylated forms of Siz1 were only slightly modulated in the WT strain. Finally, to show that nuclear accumulated Siz1 is indeed an in vivo STUbL target once the cell enters mitosis, we performed a cycloheximide chase of Siz1 in a *msn5Δslx5Δ strain*. Consistent with our prediction, Siz1 was stabilized in the *slx5Δmsn5Δ* double mutant but not the *msn5Δ* mutant (Figure 7C). Furthermore, Siz1 sumoylation in the *slx5Δmsn5Δ* double mutant was maintained through the entire cycloheximide chase time course, whereas all forms of Siz1 were rapidly degraded in the *msn5Δ* mutant.

Whether phosphorylation is solely required for Siz1's nuclear export, precedes its sumoylation, or promotes other aspects of Siz1 function is not yet clear. Of importance, our data reveal for the first time the functional interplay between SUMO E3 ligases and SUMO-targeted ubiquitin ligases. In summary, this STUbL-dependent regulation of nuclear localized Siz1 (see model in Figure 7D) may work in cooperation with other pathways to prevent the accumulation of specific nuclear SUMO conjugates that interfere with cell cycle progression or other vital processes.

DISCUSSION

We conducted an extensive structure–function analysis of the yeast STUbL subunit Slx5. Our data suggest that Slx5 consists of distinct and partially overlapping domains involved in its self-association and its interactions with Slx8 and yeast SUMO. We also began the functional dissection of a novel Slx5 interactor and STUbL target, the SUMO E3 ligase Siz1.

In our structure–function analysis of Slx5 we identified a new domain with an apparent role in nuclear localization of this STUbL subunit. Specifically, we observed that a GFP-tagged fragment of Slx5, Slx5(207–310), is enriched in the nucleus (Figure 1). Of importance, Slx5(207–310) contains an arginine-rich region (207–**RR**IAE**R**Q**RR**–215), and similar features in other proteins have been implicated in protein dimerization, nuclear transport, interaction with SH3 domain–containing proteins, and recognition of RNA hairpins (Hibbard and Sandri-Goldin, 1995; Fagerlund *et al.*, 2002; Barylko *et al.*, 2010). A conserved arginine-rich region has also been described in the human STUbL orthologue RNF4, and it has been suggested that this domain may be involved in detecting ATM-phosphorylated proteins (Kuo et al., 2012). Using a second construct that removes additional residues of the arginine cluster, Slx5(Δ189–260), we find reduced nuclear localization. Therefore, based on our data, it is possible that this domain of the STUbL subunit Slx5 is somehow involved in nuclear localization or retention. It is important to note that the same domain is also required for the two-hybrid interaction of Slx5 with other Slx5 molecules. However, the functional relevance of this interaction requires further investigation.

Unlike Slx5, Siz1 shows a cell cycle–dependent localization pattern. Nuclear-localized Siz1 becomes phosphorylated at G2/M, is concomitantly exported, and then associates with septins at the bud neck of dividing cells (Johnson and Gupta, 2001). Elegant work by Makhnevych *et al.* (2007) showed that Msn5, a karyopherin that transports phosphorylated cargoes, is involved in nuclear export of Siz1 and that this export is required for septin sumoylation. Therefore Siz1 may contain a nuclear export signal that depends on phosphorylation to be recognized by Msn5 (for comparison see DeVit and Johnston, 1999). Of interest, our work raises the possibility that Siz1 phosphorylation may also be a prelude to STUbL-mediated degradation, and we are exploring this possibility. The mammalian Siz1 orthologue PIAS1, which is phosphorylated by casein kinase 2, was recently found to contain a phosphoregulated SIM module. This phosphoregulated SIM does not appear to affect the sumoylation or turnover of PIAS1 but is required to modulate the activity of specific transcription factors (Stehmeier and Muller, 2009). A bona fide SIM also exists at position 484–491 of Siz1, but we have not yet determined whether it constitutes a phosphoregulated SIM module (Uzunova *et al.*, 2007).

One of the most intriguing implications of this work is that STUbLs can regulate an important SUMO E3 ligase. In vitro and in

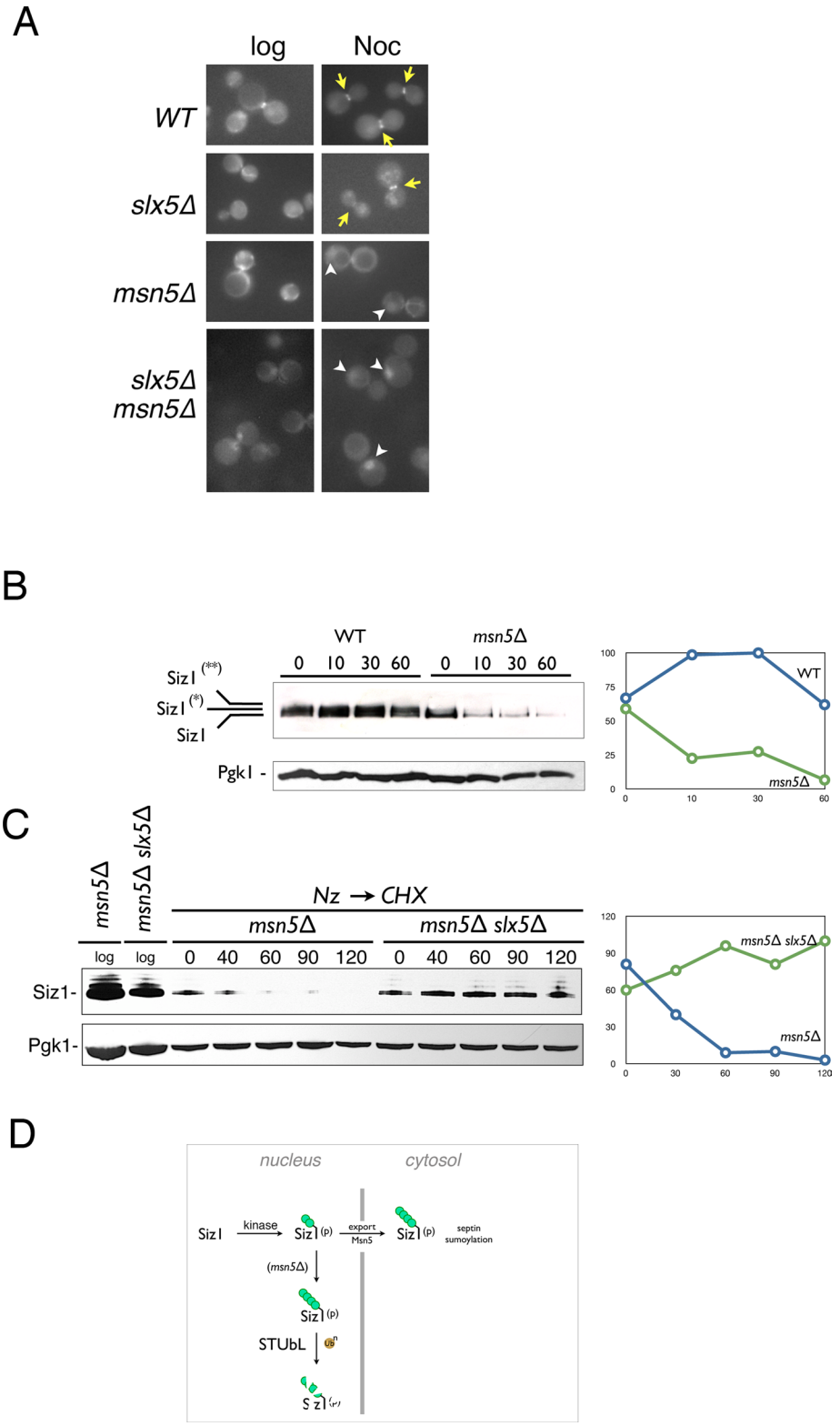

FIGURE 7: Slx5 modulates the levels of Siz1 in the nucleus. (A) WT (YOK2738), *slx5Δ* (YOK2751), *msn5Δ* (YOK2624), and *msn5Δslx5Δ* (YOK2735) strains expressing Siz1-GFP as the only copy of this SUMO ligase were imaged during logarithmic growth (log; left) or after nocodazole-induced G2/M arrest (Noc; right). The localization of Siz1-GFP at septins is indicated with yellow arrows, and the localization of nuclei in *msn5Δ* and *msn5Δslx5Δ* strains is indicated with white arrowheads. (B) Siz1 is rapidly degraded in an *msn5Δ* mutant. Isogenic WT (YOK 2397) and *msn5Δ* (YOK 2514) strains expressing endogenous full-length Siz1-myc were grown overnight in yeast extract/peptone/dextrose (YPD) medium. Cells in logarithmically grown cultures were arrested with nocodazole. G2/M-arrested cells, 10 OD units, were pelleted, washed, and resuspended in fresh YPD medium without nocodazole containing 25 µg/ml cycloheximide. Subsequently, protein extracts of 2.5 OD units of cells were prepared at the indicated time points (0, 10, 30, 60 min) before Western blotting to detect Siz1-myc. Siz1 levels were normalized against the Pgk1 loading control and graphed on the right. (C) A deletion of *SLX5* stabilizes Siz1 in an *msn5Δ* mutant. Isogenic *msn5Δ* and *msn5Δslx5Δ* strains expressing Siz1-myc from LEU2/CEN plasmid pRS315 were grown overnight in selective media. Cells in logarithmically grown cultures were arrested with nocodazole and benomyl. G2/M-arrested cells, 22 OD units, were pelleted, washed, and resuspended in fresh YPD medium without nocodazole containing 25 µg/ml cycloheximide. Subsequently, protein extracts of 2 OD units of cells were prepared at the indicated time points (0, 40, 60, 90, 120 min) before Western blotting to detect Siz1-myc and Pgk1 proteins. The first two lanes, msn5Δ (log) and msn5Δslx5Δ (log), are overloaded to show SUMO adducts of Siz1 in these strains. Siz1 levels were normalized against the Pgk1 loading control and graphed on the right. Siz1 protein levels, normalized to the Pgk1 control, were determined using a C-DiGit Western blot scanner (Li-COR, Lincoln, NE) and Image Studio software (Li-COR) and are shown below each time point. (D) Model of a STUbL-dependent nuclear degradation pathway of sumoylated Siz1. At the onset of mitosis nuclear Siz1 becomes autosumoylated (green circles) and phosphorylated (p) via an unknown kinase. Phosphorylated Siz1 may be subject to Msn5-mediated nuclear export to facilitate septin sumoylation in the cytosol. Sumoylated Siz1 that remains in the nucleus as the cell enters mitosis (in our experiments this was accomplished through deletion of *MSN5*) is subject to STUbL-mediated ubiquitylation (circle labeled Ub) and degradation. Other non–STUbL-dependent pathways for the regulation of Siz1 activity and levels may exist, and the exact structures of the Siz1 conjugates are not known.

vivo we detect robust ubiquitylation of a truncated Siz1 construct, albeit only with monoubiquitin and diubiquitin (Figure 5A). Similar to other STUbL substrates, our in vitro modification was also not dependent on prior sumoylation of Siz1 (Xie *et al.*, 2007, 2010). The same truncated Siz1 construct is also ubiquitylated in vivo, and this modification depends on *SLX5* (Figure 5B). In vivo, sumoylation may be a prerequisite, because our preliminary experiments suggest that a RING mutant of this Siz1(Siz1$^{(C377S\ H379A)}$) truncation fails to be ubiquitylated (N.P. and O.K., unpublished observations). Ultimately our data suggest that nuclear-localized Siz1 interacts with Slx5, is degraded in a

STUbL-dependent manner, and accumulates sumoylated adducts of Siz1 when *SLX5* is absent (Figure 7C). These sumoylated adducts of Siz1 may be retained in nuclei of *slx5Δ* cells, because we find a ~20% reduction of Siz1 localization to the septin ring when cells are arrested in nocodazole (C.E., J.W.W., and O.K., unpublished observations). However, another possibility is that autosumoylation of Ubc9, which was recently shown to negatively affect septin sumoylation (Ho *et al.*, 2011), is increased in *slx5Δ*.

Are there nuclear versus cytosolic STUbL functions? Slx5 is a nuclear protein, and there is no evidence that it functionally interacts with sumoylated proteins in the cytosol. Only the truncated Slx5 protein lacking a domain involved in nuclear localization and putative dimerization, Slx5(1–207), associates with the sumoylated septin ring in G2/M-arrested cells. Although not physiologically relevant, this helps to delineate a domain involved in nuclear localization of Slx5 and shows which SIMs are involved in targeting the Slx5/Slx8 STUbL. Other cytosolic proteins are known to use a SUMO-binding strategy to be recruited to the septin ring in a cell cycle–dependent manner (Elmore *et al.*, 2011). Is it possible that the various yeast STUbLs are separated into distinct cellular compartments? For example, Slx5/Slx8 may function in the nucleus, whereas sumoylated proteins in the cytosol are degraded by other STUbLs. Consistent with this hypothesis, the STUbL protein Ris1 relocalizes to the cytosol upon replication stress, and other recent work suggests that Ris1 targets the microtubule-associated protein Pac1 in the cytosol (Alonso *et al.*, 2012; Tkach *et al.*, 2012).

In conclusion, we predict that the degradation of Siz1 by Slx5/Slx8 plays an important physiological role in reducing nuclear SUMO E3 ligase activity as the cell enters mitosis. This novel process likely works in parallel to the mitotic nuclear export pathway of Siz1 and may help to prevent the accumulation of specific nuclear SUMO conjugates that interfere with cell cycle progression (see *Introduction*). Considering that Slx5 and Siz1 are evolutionarily conserved proteins, we predict that the STUbL-mediated regulation of SUMO-E3 ligases extends to RNF4 and PIAS proteins in mammalian cells. Indeed, our preliminary analysis indicates that RNF4 can interact with PIAS1 in yeast two-hybrid and pull-down assays (Kerscher, Westerbeck, and Semmes, unpublished observations). It will be interesting to determine whether RNF4 affects the turnover of PIAS1 in mammalian cells. This would further support the emerging theme of interconnection and interdependence of SUMO and ubiquitin systems.

MATERIALS AND METHODS

Yeast strains, media, and plasmids

Yeast strains and plasmids used in this study are listed in Table 1. Unless otherwise noted, yeast media preparation and manipulation of yeast cells were performed as previously reported (Guthrie and Fink, 2002). All strains were grown at 30°C unless otherwise noted.

Cell synchronization and drug treatments

Where indicated, yeast cells were synchronized in G2/M phase by incubating logarithmically grown cells in 15 μg/ml nocodazole (358240500; Acros Organics) for 3 h at 30°C. For cycloheximide chase experiments, 25 μg/ml cycloheximide (C7698; Sigma-Aldrich, St. Louis, MO) was added to G2/M-arrested cells. We harvested 2.5 OD units of cells at the indicated time points. Cells were arrested in S phase by addition of 0.1 M hydroxyurea (H8627; Sigma-Aldrich) and incubation at 30°C for 3 h.

Cloning and epitope tagging of yeast genes

Slx5 and Slx5 domains under control of its endogenous promoter were PCR amplified from yeast genomic DNA and placed in-frame with a carboxy-terminal GFP tag in CEN/LEU2 plasmid pAA3 (Sesaki and Jensen, 1999; Cook *et al.*, 2009). Nuclear versus cytosolic localization of GFP-tagged constructs was confirmed using 4′,6-diamidino-2-phenylindole. For galactose-inducible expression of Siz1(Δ440) in yeast, the open reading frame (ORF) was PCR amplified and cloned into the pCR8/GW/TOPO entry vector (Life Technologies, Grand Island, NY) and then recombined into pAG425GAL-ccdB-HA/LEU2 (plasmid 14249; Addgene, Cambridge MA), forming Gal-Siz1Δ440-HA/LEU2/2 μ (plasmid BOK795). For in vivo pull-down assays a plasmid expressing GST-tagged Slx5 (YSC4515-202484078) was purchased from the Thermo Scientific Life Science Research Yeast (Thermo Scientific, Pittsburgh PA) GST-tagged ORF Collection (formerly Open Biosystems). For two-hybrid constructs, ORFs or truncations of the indicated genes were PCR amplified, homologously recombined into gapped pOAD and pOBD2 vectors, and transformed into AH109 (YOK1220) strains as specified (Yeast Resource Center, University of Washington, Seattle, WA). Two-hybrid interactions were scored on dropout media lacking adenine as specified in the Clontech Yeast Protocols Handbook (protocol PT3024-1; Clontech Laboratories). Chromosomal tagging and gene deletions in yeast were carried out by PCR-based homologous recombination (Longtine *et al.*, 1998). Strain YOK821 (*slx5Δ*) was used to epitope tag *SIZ1* with a 13-myc epitope tag. Briefly, primers OOK663 and OOK662 were used to amplify the 13xmyc-TADH1-His3MX6 cassette with 40 base pairs of *SIZ1* sequence homology from the plasmid pFA6a-13myc-His3MX6 (Longtine *et al.*, 1998). PCR amplification was carried out using the Phusion High-Fidelity PCR kit (E0553S; New England BioLabs, Ipswich, MA) with dimethylsulfoxide and high-GC buffer as recommended by the manufacturer. For transformation, 6.5 μg of purified SIZ1-13myc-His3MX6 PCR product was combined with 4 OD units of competent *slx5Δ* (YOK821) cells, incubated for 30 min at 30°C, heat shocked at 42°C for 30 min, and plated on SD –His dropout. Resulting colonies were screened by Western blotting using an anti-myc antibody. Subsequently, the *SIZ1-myc slx5Δ* strain (YOK2264) was backcrossed to YOK819 to obtain *SIZ1-myc SLX5(WT)* progeny (YOK2286). An amplicon of SIZ1-13myc was also cloned into a Gateway-compatible pRS315 plasmid. The *msn5*-null mutant was constructed by introducing a hygromycin deletion cassette with 78–base pair flanking sequence homology to msn5 gene upstream and downstream region. The primer pairs for amplification of a *MSN5*-specific hygromycin deletion cassette in plasmid pAG32 were OOK763 and OOK764 and for re-PCR were OOK767 (*MSN5*[–78 to –19] and OOK768 (*MSN5*[+3692–3751]). All primer sequences are available upon request.

Recombinant proteins

For the in vitro ubiquitylation and pull-down assays recombinant MBP-Slx5, MBP-Slx8, and His6-Ubc4 were prepared as previously reported (Xie *et al.*, 2007; Fryrear *et al.*, 2012). Recombinant Siz1(Δ440) was expressed from plasmid pT-77-SIZ1Δ440-His obtained from Addgene (plasmid 16087; Takahashi and Kikuchi, 2005). CUP1-driven UbiG76A and mycUbi-G76A plasmids expressing deubiquitylation-resistant mutants of ubiquitin were a gift from Tommer Ravid (The Hebrew University of Jerusalem).

Pull-down assays, affinity purification, and protein extracts

MBP-Slx5, MBP-Slx8, and T7-Siz1Δ440 were overexpressed in BL21(DE3) or *R cells by isopropyl-β-D-thiogalactoside induction as previously described (Xie *et al.*, 2007). We combined 50 OD units of cells overexpressing either MBP-Slx5 or MBP-Slx8 with 50 OD units of cells overexpressing T7-Siz1Δ440. We also collected 50 OD units of cells overexpressing T7-Siz1Δ440. Whole-cell protein extracts

Name	Pertinent genotype or background	Plasmid or construction	Reference
MHY500 (YOK819)	Mata his3-Δ200 leu2-3, 112 ura3-52 lys2-801trp1-1gal2		Li and Hochstrasser (2003)
MHY501 (YOK820)	Matα his3-Δ200 *leu2-3, 112 ura3-52 lys2-801trp1-1 gal2*		
BY4741 (YOK1322)	MATa leu2Δ0 met15Δ0 ura3Δ0		Brachmann *et al.* (1998)
JD52 (YOK2062)	MATa ura3-52 his3-Δ200 leu2-3112 trp1-Δ63 lys2-801		Dohmen *et al.* (1995)
AH109 (YOK1220)	*MATa, trp1-901, leu2-3, 112, ura3-52*, his3-200, gal4Δ, gal80Δ, LYS2::GAL1UAS-GAL-1TATA-HIS3, GAL2UAS-GAL2TATA-ADE2, URA3::MEL1UASMEL1TATA-lacZ, MEL1		Cat. No. 630444; Clontech, Mountain View, CA
YOK1369	*BY4741 (YOK1322)*	SLX5(1-50)-GFP/LEU2 (BOK514)	This study
YOK1370	*BY4741 (YOK1322)*	SLX5(1-104)-GFP/LEU2 (BOK515)	This study
YOK1372	*BY4741 (YOK1322)*	SLX5(1-310)-GFP/LEU2 (BOK517)	This study
YOK1373	*BY4741 (YOK1322)*	SLX5(1-414)-GFP/LEU2 (BOK518)	This study
YOK1374	*BY4741 (YOK1322)*	SLX5(1-517)-GFP/LEU2 (BOK519)	This study
YOK1375	*BY4741 (YOK1322)*	SLX5(1-207)-GFP/LEU2 (BOK507)	This study
YOK1830	*MHY500*	SLX5(208-310)-GFP/LEU2 (BOK637)	This study
YOK1408	*AH109*	SLX5(1-104)-BD/TRP; SLX5-AD/LEU2 (BOK289)	This study
YOK1411	*AH109*	SLX5(1-207)-BD/TRP; SLX5-AD/LEU2 (BOK289)	This study
YOK1414	*AH109*	SLX5(1-310)-BD/TRP; SLX5-AD/LEU2 (BOK289)	This study
YOK1417	*AH109*	SLX5(1-414)-BD/TRP; SLX5-AD/LEU2 (BOK289)	This study
YOK1420	*AH109*	SLX5(1-517)-BD/TRP; SLX5-AD/LEU2 (BOK289)	This study
YOK1423	*AH109*	SLX5(51-620)-BD/TRP; SLX5-AD/LEU2 (BOK289)	This study
YOK1425	*AH109*	SLX5(105-620)-BD/TRP; SLX5-AD/LEU2 (BOK289)	This study
YOK1428	*AH109*	SLX5(208-620)-BD/TRP; SLX5-AD/LEU2 (BOK289)	This study
YOK1431	*AH109*	SLX5(311-620)-BD/TRP; SLX5-AD/LEU2 (BOK289)	This study
YOK1434	*AH109*	SLX5(415-620)-BD/TRP; SLX5-AD/LEU2 (BOK289)	This study
YOK1437	*AH109*	SLX5(1-104)-BD/TRP; SLX8-AD/LEU2 (BOK311)	This study
YOK1440	*AH109*	SLX5(1-207)-BD/TRP; SLX8-AD/LEU2 (BOK311)	This study
YOK1443	*AH109*	SLX5(1-310)-BD/TRP; SLX8-AD/LEU2 (BOK311)	This study
YOK1446	*AH109*	SLX5(1-414)-BD/TRP; SLX8-AD/LEU2 (BOK311)	This study
YOK1449	*AH109*	SLX5(1-517)-BD/TRP; SLX8-AD/LEU2 (BOK311)	This study

TABLE 1: Strains and plasmids used in this study.

Continues

Name	Pertinent genotype or background	Plasmid or construction	Reference
YOK1452	*AH109*	SLX5(51-620)-BD/TRP; SLX8-AD/LEU2 (BOK311)	This study
YOK1455	*AH109*	SLX5(105-620)-BD/TRP; SLX8-AD/LEU2 (BOK311)	This study
YOK1458	*AH109*	SLX5(208-620)-BD/TRP; SLX8-AD/LEU2 (BOK311)	This study
YOK1461	*AH109*	SLX5(311-620)-BD/TRP; SLX8-AD/LEU2 (BOK311)	This study
YOK1464	*AH109*	SLX5(415-620)-BD/TRP; SLX8-AD/LEU2 (BOK311)	This study
YOK1467	*AH109*	SLX5-BD/TRP (BOK440); SlX5-AD/LEU2 (BOK289)	This study
YOK1470	*AH109*	SLX5-BD/TRP (BOK440); SLX8-AD/LEU2 (BOK311)	This study
YOK1518	*AH109*	SLX5-BD/TRP (BOK440); SMT3-AD/LEU2 (BOK571)	This study
YOK1547	*AH109*	SLX5(1-50)-BD/TRP SMT3-AD/LEU2 (BOK571)	This study
YOK1550	*AH109*	SLX5(1-104)-BD/TRP; SMT3-AD/LEU2 (BOK571)	This study
YOK1553	*AH109*	SLX5(1-207)-BD/TRP; SMT3-AD/LEU2 (BOK571)	This study
YOK1556	*AH109*	SLX5(1-310)-BD/TRP; SMT3-AD/LEU2 (BOK571)	This study
YOK1559	*AH109*	SLX5(1-414)-BD/TRP; SMT3-AD/LEU2 (BOK571)	This study
YOK1562	*AH109*	SLX5(1-517)-BD/TRP; SMT3-AD/LEU2 (BOK571)	This study
YOK1565	*AH109*	SLX5(51-620)-BD/TRP; SMT3-AD/LEU2 (BOK571)	This study
YOK1568	*AH109*	SLX5(311-620)-BD/TRP; SMT3-AD/LEU2 (BOK571)	This study
YOK1571	*AH109*	SLX5(208-620)-BD/TRP; SMT3-AD/LEU2 (BOK571)	This study
YOK1574	*AH109*	SLX5(311-620)-BD/TRP; SMT3-AD/LEU2 (BOK571)	This study
YOK1577	*AH109*	SLX5(415-620)-BD/TRP; SMT3-AD/LEU2 (BOK571)	This study
YOK1580	*AH109*	SLX5(518-620)-BD/TRP; SMT3-AD/LEU2 (BOK571)	This study
YOK1583	*AH109*	SLX5(518-620)-BD/TRP; SLX8-AD/LEU2 (BOK311)	This study
YOK1586	*AH109*	SLX5(518-620)-BD/TRP; SLX5-AD/LEU2 (BOK289)	This study
YOK1589	*AH109*	SLX5(1-50)-BD/TRP SLX8-AD/LEU2 (BOK311)	This study
YOK1592	*AH109*	SLX5(1-50)-BD/TRP SLX5-AD/LEU2 (BOK289)	This study
YOK1595	*AH109*	SLX5-BD/TRP (BOK440); SIZ1-AD/LEU2 (BOK582)	This study
YOK1621	*AH109*	SLX5(1-50)-BD/TRP SIZ1-AD/LEU2 (BOK582)	This study

TABLE 1: Strains and plasmids used in this study.

Continues

Name	Pertinent genotype or background	Plasmid or construction	Reference
YOK1625	*AH109*	SLX5(1-104)-BD/TRP; SIZ1-AD/LEU2 (BOK582)	This study
YOK1627	*AH109*	SLX5(1-207)-BD/TRP; SIZ1-AD/LEU2 (BOK582)	This study
YOK1630	*AH109*	SLX5(1-310)-BD/TRP; SIZ1-AD/LEU2 (BOK582)	This study
YOK1633	*AH109*	SLX5(1-414)-BD/TRP; SIZ1-AD/LEU2 (BOK582)	This study
YOK1636	*AH109*	SLX5(1-517)-BD/TRP; SIZ1-AD/LEU2 (BOK582)	This study
YOK1639	*AH109*	SLX5(51-620)-BD/TRP; SIZ1-AD/LEU2 (BOK582)	This study
YOK1642	*AH109*	SLX5(311-620)-BD/TRP; SIZ1-AD/LEU2 (BOK582)	This study
YOK1645	*AH109*	SLX5(208-620)-BD/TRP; SIZ1-AD/LEU2 (BOK582)	This study
YOK1648	*AH109*	SLX5(311-620)-BD/TRP; SIZ1-AD/LEU2 (BOK582)	This study
YOK1651	*AH109*	SLX5(415-620)-BD/TRP; SIZ1-AD/LEU2 (BOK582)	This study
YOK1654	*AH109*	SLX5(518-620)-BD/TRP; SIZ1-AD/LEU2 (BOK582)	This study
YOK1796	*AH109*	SLX5(SIMAB)-BD/TRP; SLX8-AD/LEU2 (BOK311)	This study
YOK1797	*AH109*	SLX5(SIMAB)-BD/TRP; SLX8-AD/LEU2 (BOK311)	This study
YOK1798	*AH109*	SLX5(SIMAB)-BD/TRP; SLX8-AD/LEU2 (BOK311)	This study
YOK1799	*AH109*	SLX5(SIMAB)-BD/TRP (BOK627); SMT3-AD/ LEU2 (BOK571)	This study
YOK1800	*AH109*	SLX5(SIMAB)-BD/TRP(BOK627); SMT3-AD/ LEU2 (BOK571)	This study
YOK1801	*AH109*	SLX5(SIMAB)-BD/TRP(BOK627); SMT3-AD/ LEU2 (BOK571)	This study
YOK2396	*slx5::KanMX4 SIZ1-13xmyc/HIS5* in JD52	YOK 2373 transformed with *SIZ1-13xmyc/ HIS5*	This study
YOK2397	*SIZ1-13xmyc/HIS5* in JD52	YOK 2062 transformed with *SIZ1-13xmyc/ HIS5*	This study
YOK2514	*msn5::HYG SIZ1-13xmyc/HIS5* in JD52	YOK 2397 transformed with *msn5::HYG*	This study
YOK2513	*msn5::HYG, slx5::KanMX4 SIZ1-13xmyc/HIS5*	YOK 2396 transformed with *msn5::HYG*	This study
YOK3712 (MHY821)	*slx5::KANMX4*		Xie *et al*. (2007)
YOK2264	slx5Δ SIZ1-13xmyc/HIS5	MHY821 transformed with *SIZ1-13xmyc/HIS5*	This study
YOK2286	*SIZ1-13xmyc/HIS5*	MHY501 transformed with *SIZ1-13xmyc/HIS5*	This study
YOK2373	*slx5::KANMX4* in JD52	YOK2062 with integrated *slx5::KANMX4* cassette	This study
YOK2505	*msn5::HYG* in JD52	YOK2062 with integrated *msn5::HYG* cassette	This study
YOK2681	*slx5::KANMX4 msn5::HYG* in JD52	YOK2062 with integrated slx5::KANMX4 and *msn5::HYG* cassettes	This study

TABLE 1: Strains and plasmids used in this study.

Continues

Name	Pertinent genotype or background	Plasmid or construction	Reference
YOK2738	*SIZ1-GFP/HIS5* in JD52	YOK 2062 transformed with *SIZ1-GFP/HIS5*	This study
YOK2751	*slx5::KANMX4 SIZ1-GFP/HIS5* in JD52	YOK 2373 transformed with *SIZ1-GFP/HIS5*	This study
YOK2624	*msn5::HYG SIZ1-GFP/HIS5* in JD52	YOK2505 transformed with *SIZ1-GFP/HIS5*	This study
YOK2735	*slx5::KANMX4 msn5::HYG SIZ1-GFP/HIS5* in JD52	YOK2681 transformed with *SIZ1-GFP/HIS5*	This study
YOK2757	*slx5::KANMX4* in JD52	YOK2373 transformed with *SIZ1-13xmyc/LEU2* on pRS315 (BOK982)	This study
YOK2759	*msn5::HYG* in JD52	YOK2505 transformed with *SIZ1-13xmyc/LEU2* on pRS315 (BOK982)	This study
YOK2761	*slx5::KanMX4 msn5::HYG* in JD52	YOK2681 transformed with *SIZ1-13xmyc/LEU2* on pRS315 (BOK982)	This study
YOK2501	MHY3765: *MATalpha* ura3-52, lys2-801, trp1-Δ63, his3-Δ200, leu2-Δ1, ubc4::HIS3, ubc6::TRP1, alpha2::KanMX		Xie *et al*. (2010)
YOK2507	YOK2501 + *pGAL1/10-GST-Slx5*	BOK629 (GAL1/10-GST-Slx5) (Open Biosystems Yeast GST Collection) transformed into YOK2501	This study
YOK2508	YOK2501 + *pGAL1-ccdB-Siz1Δ440-HA*	BOK795 transformed into 2501	This study
YOK2509	YOK250 + *pGAL1/10-GST-Slx5; pGAL1-ccdB-Siz1Δ440-HA*	BOK629 and BOK795 transformed into YOK2501	This study
YOK2379	pYES2.1-GAL- Siz1Δ440-V5/His6-TOPO; CUP1-UbiG76A-myc in JD52	BOK794 and BOK309 transformed into YOK2062	
YOK2381	*slx5::KAN* YOK2373 + pYES2.1-GAL-Siz1Δ440-V5/His6-TOPO; CUP1-UbiG76A-myc	BOK794 and BOK309 transformed into YOK2373	

TABLE 1: Strains and plasmids used in this study. Continued

were then isolated and passed over a column containing amylose resin (E8021L; New England BioLabs). Proteins bound to the amylose resin were eluted with 1× LDS Sample Buffer (NP0007; Life Technologies) and analyzed by Western blotting as described later. To determine whether Slx5 and Siz1 interacted in vivo, GAL1/10-GST-Slx5 (BOK 629, Open Biosystems Yeast GST Collection YSC4515-202484078), pAG425-GAL1-ccdB-Siz1(Δ440)-HA (BOK795), or both GST-Slx5 and Siz1(Δ440)-HA were transformed into *ubc4Δ ubc6Δ* cells (YOK2501, Xie *et al*., 2010) to form YOK2507, YOK2508, and YOK2509, respectively. Copurification experiments were done as described in Szymanski and Kerscher (2013). Transformants were grown in 33 ml of the appropriate selective media containing 2% sucrose until mid–log phase (OD_{600} = 0.8–1.0). At this point, 17 ml of 3× yeast extract peptone (YEP) with 6% galactose was added to each culture, for a final concentration of 1× YEP and 2% galactose in a final volume of 50 ml. Cells were allowed to grow for another 6 h before harvesting. We washed 200 OD units worth of yeast cells with 1× ice-cold phosphate-buffered saline plus 1× protease inhibitor cocktail (1860932; Thermo Scientific), snap froze them in liquid nitrogen, and stored them at −80°C until further use. To extract proteins, frozen cell pellets were lysed in 500 µl of HNT buffer (50 mM 4-(2-hydroxyethyl)-1-piperazineethanesulfonic acid [HEPES] at pH 7.3, 200 mM NaCl, 1% Triton X-100) containing 25 mM *N*-ethylmaleimide (NEM), 1 mM sodium orthovanadate, and 1× protease inhibitor cocktail (G6521; Promega, Madison, WI), and 200 µl of acid-washed beads (425–600 µm; Sigma-Aldrich) were placed in an Omni Bead Ruptor 24 (six 20-s pulses with 1 min on slushy ice between each pulse). The lysate was clarified by centrifugation at 15,000 rpm for 15 min at 4°C. We added 100 µl of clarified lysate (corresponding to 20 OD units) to 100 µl of immobilized glutathione agarose (15160; Thermo Scientific) that had been equilibrated with HNT buffer and increased the final volume to 1 ml with HNT buffer plus 25 mM NEM, 1 mM sodium orthovanadate, and 1× protease inhibitor cocktail (1860932; Thermo Scientific). Extracts were rotated top over bottom with the glutathione agarose for 2.5 h at 4°C. Agarose beads were then washed five times with HNT buffer. We saved 100 µl of the flowthrough and precipitated proteins by addition of 1 ml of 20% trichloroacetic acid (TCA). Glutathione agarose–bound proteins were eluted by top-over-bottom rotation with 100 µl of elution buffer (50 mM HEPES at pH 7.3, 200 mM NaCl, 10 mM reduced glutathione [120000010; Acros Organics]) for 5 min. Three elutions were performed and pooled before analysis of proteins by SDS–PAGE and Western blotting. The $Ubi^{(G76A)}$ construct was induced as previously reported (Ravid and Hochstrasser, 2007), and extracts were prepared as listed except that 20 µM MG132 was added to the cultures and anti–V5-agarose was used for immunoprecipitations (A7345; Sigma-Aldrich).

Preparation of whole-cell yeast extracts, gel electrophoresis, and Western blotting

Whole-cell yeast extracts were prepared by TCA glass bead lysis. Whole-cell protein extracts corresponding to ~0.2 OD unit were separated on a precast NuPAGE Novex 4–12% Bis-Tris gels (NP0321; Life Technologies) or home-made 8% Tris-glycine gels. After separation, proteins were transferred to polyvinylidene difluoride membrane (IPVH00010; Millipore, Billerica, MA) for 25 min at 19 V. Blots were

blocked in TBS (150 mM NaCl, 50 mM Tris-HCl at pH 7.4) containing 4% milk for 1 h and then incubated in 4% milk containing primary antibody overnight, followed by incubation with secondary antibodies for 1–3 h at ambient temperature. After antibody incubations, blots were extensively washed in TBS plus 0.1% Tween 20 (TBST). Anti-GST antibody (1:5000 dilution, ab6613; Abcam), anti-hemagglutinin (HA) antibody (1:10,000, ab9110; Abcam), anti-T7 (1:10,000 dilution, 69522-3; Novagen [EMD Millipore], Billerica, MA), anti-myc (1:5000, MMS-150R; Covance, Princeton, NJ), anti-Pgk (1:10,000, A6457; Life Technologies), anti-GST (1:5000, ab6613, Abcam), anti-FLAG (1:10,000, F3165; Sigma-Aldrich), anti-mouse horseradish peroxidase (HRP; 1:15,000, ab9740; Abcam), and anti-rabbit HRP (1:20,000, ab6721; Abcam). Proteins were visualized on film using enhanced chemiluminescence substrate (Immobilon Western ECL substrate WBKL S0 100; Millipore).

In vitro ubiquitylation reactions

Sizing and quantitation of enzymes and substrates used in our in vitro ubiquitylation assays were performed with a Protein 230 kit on the Agilent 2100 Bioanalyzer according to the manufacturer's instructions. The 10× ubiquitylation buffer, E1 enzyme (Uba1), ATP, and 20× ubiquitin were provided in a commercial ubiquitylation kit (Enzo). Ubiquitylation buffer, inorganic pyrophosphatase (IPP; 100 U/ml), dithiothreitol (DTT; 50 µM), E1 (Uba1), E2 (Ubc4), and E3 enzyme (Slx5-Slx8) were combined with purified substrate protein (T7-Siz1Δ440) and ubiquitin as previously reported (Xie *et al.*, 2007). Reactions totaled 27 µl and were incubated in a 30°C heat block for 3 h. Molar ratios of components in the STUbL ubiquitylation reactions were as follows (µM): E1(Uba1), 0.1; E2(Ubc4), 0.4; E3 (Slx5/Slx8), 0.12 each; and substrate (Siz1Δ440), 0.03. Reactions were stopped by adding an equal volume of SUTEB sample buffer (0.01% bromophenol blue, 10 mM EDTA, 1% SDS, 50 mM Tris at pH 6.8, 8 M urea) containing DTT (5 µl of 1 M DTT/1 ml SUTEB sample buffer). Protein products were boiled in a 65°C heat block for 10 min, frozen in liquid nitrogen, stored at –80°C, and analyzed by Western blot as described.

Fluorescence microscopy

Images of live cells were collected using a Zeiss Axioskop fitted with a Retiga SRV camera (Q-imaging), i-Vision software (BioVision Technologies), and a Uniblitz shutter assembly (Rochester, NY). Pertinent filter sets for the applications include CZ909 (GFP), XF114-2 (CFP), and XF104-2 (YFP; Chroma Technology Group, Bellows Falls, VT). Where applicable, images were normalized using i-Vision software and pseudocolored and adjusted using Photoshop software (Adobe Systems, San Jose, CA).

ACKNOWLEDGMENTS

We thank all members of the Kerscher lab for their support, especially Nora Foegeding for help with plasmid constructions and Zac Elmore, Jeff Hollomon, and Andrew Halleran for insightful discussions. We are also indebted to Tamara Golden, Diane Shakes, Liz Allison, and Gloria Driessnack for critical reading and/or edits of the manuscript and Matthias Leu for help with statistical analyses. We thank Mark Hochstrasser, Eric Rubenstein, Erica Johnson, Helle Ulrich, Anthony Antonellis, and Tommer Ravid for strains, plasmids, and reagents. This work was supported by National Science Foundation Grant 1051970 (to O.K.), William & Mary Howard Hughes Undergraduate Summer Research Fellowships or Travel Awards (to E.S., C.E., and B.C.M.), an ALSAM fellowship (to B.C.M.), a William and Mary Arts and Sciences Graduate Research Grant (to J.W.), and a NASA Virginia Space Grant Consortium Grant (to J.W.).

REFERENCES

Alonso A, D'Silva S, Rahman M, Meluh PB, Keeling J, Meednu N, Hoops HJ, Miller RK (2012). The yeast homologue of the microtubule-associated protein Lis1 interacts with the sumoylation machinery and a SUMO-targeted ubiquitin ligase. Mol Biol Cell 23, 4552–4566.

Barylko B, Wang L, Binns DD, Ross JA, Tassin TC, Collins KA, Jameson DM, Albanesi JP (2010). The proline/arginine-rich domain is a major determinant of dynamin self-activation. Biochemistry 49, 10592–10594.

Brachmann CB, Davies A, Cost GJ, Caputo E (1998). Designer deletion strains derived from *Saccharomyces cerevisiae* S288C: a useful set of strains and plasmids for PCR-mediated gene disruption and other applications. Yeast 14, 115–132.

Bylebyl GR, Belichenko I, Johnson ES (2003). The SUMO isopeptidase Ulp2 prevents accumulation of SUMO chains in yeast. J Biol Chem 278, 44113–44120.

Cao L, Yu W, Wu Y, Yu L (2009). The evolution, complex structures and function of septin proteins. Cell Mol Life Sci 66, 3309–3323.

Cheng C-H, Lo Y-H, Liang S-S, Ti S-C, Lin F-M, Yeh C-H, Huang H-Y, Wang T-F (2006). SUMO modifications control assembly of synaptonemal complex and polycomplex in meiosis of *Saccharomyces cerevisiae*. Genes Dev 20, 2067–2081.

Cook CE, Hochstrasser M, Kerscher O (2009). The SUMO-targeted ubiquitin ligase subunit Slx5 resides in nuclear foci and at sites of DNA breaks. Cell Cycle 8, 1080–1089.

Deshaies RJ, Joazeiro CAP (2009). RING domain E3 ubiquitin ligases. Annu Rev Biochem 78, 399–434.

DeVit MJ, Johnston M (1999). The nuclear exportin Msn5 is required for nuclear export of the Mig1 glucose repressor of *Saccharomyces cerevisiae*. Curr Biol 9, 1231–1241.

Dohmen RJ, Stappen R, McGrath JP, Forrová H, Kolarov J, Goffeau A, Varshavsky A (1995). An essential yeast gene encoding a homolog of ubiquitin-activating enzyme. J Biol Chem 270, 18099–18109.

Douglas LM, Alvarez FJ, McCreary C, Konopka JB (2005). Septin function in yeast model systems and pathogenic fungi. Eukaryotic Cell 4, 1503–1512.

Elmore ZC, Donaher M, Matson BC, Murphy H, Westerbeck JW, Kerscher O (2011). Sumo-dependent substrate targeting of the SUMO protease Ulp1. BMC Biol 9, 74.

Fagerlund R, Mélen K, Kinnunen L, Julkunen I (2002). Arginine/lysine-rich nuclear localization signals mediate interactions between dimeric STATs and importin alpha 5. J Biol Chem 277, 30072–30078.

Fryrear KA, Durkin SS, Gupta SK, Tiedebohl JB, Semmes OJ (2009). Dimerization and a novel Tax speckled structure localization signal are required for Tax nuclear localization. J Virol 83, 5339–5352.

Fryrear KA, Guo X, Kerscher O, Semmes OJ (2012). The Sumo-targeted ubiquitin ligase RNF4 regulates the localization and function of the HTLV-1 oncoprotein Tax. Blood 119, 1173–1181.

Garza R, Pillus L (2013). STUbLs in chromatin and genome stability. Biopolymers 99, 146–154.

Geoffroy M-C, Hay RT (2009). An additional role for SUMO in ubiquitin-mediated proteolysis. Nat Rev Mol Cell Biol 10, 564–568.

Guthrie C, Fink GR (2002). Guide to Yeast Genetics and Molecular and Cell Biology, San Diego, CA: Academic Press.

Guzzo CM, Berndsen CE, Zhu J, Gupta V, Datta A, Greenberg RA, Wolberger C, Matunis MJ (2012). RNF4-dependent hybrid SUMO-ubiquitin chains are signals for RAP80 and thereby mediate the recruitment of BRCA1 to sites of DNA damage. Sci Signal 5, ra88.

Guzzo CM, Matunis MJ (2013). Expanding SUMO and ubiquitin-mediated signaling through hybrid SUMO-ubiquitin chains and their receptors. Cell Cycle 12, 1015–1017.

Hayes AP, Sevi LA, Feldt MC, Rose MD, Gammie AE (2009). Reciprocal regulation of nuclear import of the yeast MutSalpha DNA mismatch repair proteins Msh2 and Msh6. DNA Repair (Amst) 8, 739–751.

Hibbard MK, Sandri-Goldin RM (1995). Arginine-rich regions succeeding the nuclear localization region of the herpes simplex virus type 1 regulatory protein ICP27 are required for efficient nuclear localization and late gene expression. J Virol 69, 4656–4667.

Ho C-W, Chen H-T, Hwang J (2011). UBC9 autosumoylation negatively regulates sumoylation of septins in *Saccharomyces cerevisiae*. J Biol Chem 286, 21826–21834.

Hodgins RR, Ellison KS, Ellison MJ (1992). Expression of a ubiquitin derivative that conjugates to protein irreversibly produces phenotypes consistent with a ubiquitin deficiency. J Biol Chem 267, 8807–8812.

Ii T, Mullen JR, Slagle CE, Brill SJ (2007). Stimulation of in vitro sumoylation by Slx5-Slx8: evidence for a functional interaction with the SUMO pathway. DNA Repair (Amst) 6, 1679–1691.

Johnson ES, Blobel G (1999). Cell cycle-regulated attachment of the ubiquitin-related protein SUMO to the yeast septins. J Cell Biol 147, 981–994.
Johnson ES, Gupta AA (2001). An E3-like factor that promotes SUMO conjugation to the yeast septins. Cell 106, 735–744.
Kerscher O (2007). SUMO junction-what's your function? New insights through SUMO-interacting motifs. EMBO Rep 8, 550–555.
Kerscher O, Felberbaum R, Hochstrasser M (2006). Modification of proteins by ubiquitin and ubiquitin-like proteins. Annu Rev Cell Dev Biol 22, 159–180.
Kuo CY, Shieh C, Cai F, Ann DK (2012). Coordinate to guard: crosstalk of phosphorylation, sumoylation, and ubiquitylation in DNA damage response. Front Oncol 1, 61.
Kusch J, Meyer A, Snyder MP, Barral Y (2002). Microtubule capture by the cleavage apparatus is required for proper spindle positioning in yeast. Genes Dev 16, 1627–1639.
Li S-J, Hochstrasser M (1999). A new protease required for cell-cycle progression in yeast. Nature 398, 246–251.
Li S-J, Hochstrasser M (2000). The yeast ULP2 (SMT4) gene encodes a novel protease specific for the ubiquitin-like Smt3 protein. Mol Cell Biol 20, 2367–2377.
Li S-J, Hochstrasser M (2003). The Ulp1 SUMO isopeptidase. J Cell Biol 160, 1069–1081.
Liew CW, Sun H, Hunter T, Day CL (2010). RING domain dimerization is essential for RNF4 function. Biochem J 431, 23–29.
Lin D-Y *et al*. (2006). Role of SUMO-interacting motif in Daxx SUMO modification, subnuclear localization, and repression of sumoylated transcription factors. Mol Cell 24, 341–354.
Longtine MS, McKenzie A, Demarini DJ, Shah NG, Wach A, Brachat A, Philippsen P, Pringle JR (1998). Additional modules for versatile and economical PCR-based gene deletion and modification in *Saccharomyces cerevisiae*. Yeast 14, 953–961.
Makhnevych T, Ptak C, Lusk CP, Aitchison JD, Wozniak RW (2007). The role of karyopherins in the regulated sumoylation of septins. J Cell Biol 177, 39–49.
Mukhopadhyay D, Arnaoutov A, Dasso M (2010). The SUMO protease SENP6 is essential for inner kinetochore assembly. J Cell Biol 188, 681–692.
Mullen JR, Brill SJ (2008). Activation of the Slx5-Slx8 ubiquitin ligase by poly-small ubiquitin-like modifier conjugates. J Biol Chem 283, 19912–19921.
Mullen JR, Das M, Brill SJ (2011). Genetic evidence that polysumoylation bypasses the need for a SUMO-targeted Ub ligase. Genetics 187, 73–87.
Mullen JR, Kaliraman V, Ibrahim SS, Brill SJ (2001). Requirement for three novel protein complexes in the absence of the Sgs1 DNA helicase in *Saccharomyces cerevisiae*. Genetics 157, 103–118.
Nagai S, Dubrana K, Tsai-Pflugfelder M, Davidson MB, Roberts TM, Brown GW, Varela E, Hediger F, Gasser SM, Krogan NJ (2008). Functional targeting of DNA damage to a nuclear pore-associated SUMO-dependent ubiquitin ligase. Science 322, 597–602.
Nie M, Aslanian A, Prudden J, Heideker J, Vashisht AA, Wohlschlegel JA, Yates JR, Boddy MN (2012). Dual recruitment of Cdc48 (p97)-Ufd1-Npl4 ubiquitin-selective segregase by small ubiquitin-like modifier protein (SUMO) and ubiquitin in SUMO-targeted ubiquitin ligase-mediated genome stability functions. J Biol Chem 287, 29610–29619.
Okita YY, Nakayama KIK (2012). UPS delivers pluripotency. Cell Stem Cell 11, 728–730.
Parker JL, Ulrich HD (2012). A SUMO-interacting motif activates budding yeast ubiquitin ligase Rad18 towards SUMO-modified PCNA. Nucleic Acids Res 40, 11380–11388.
Praefcke GJK, Hofmann K, Dohmen RJ (2012). SUMO playing tag with ubiquitin. Trends Biochem Sci 37, 23–31.
Prudden J, Pebernard S, Raffa G, Slavin DA, Perry JJP, Tainer JA, McGowan CH, Boddy MN (2007). SUMO-targeted ubiquitin ligases in genome stability. EMBO J 26, 4089–4101.
Ravid T, Hochstrasser M (2007). Autoregulation of an E2 enzyme by ubiquitin-chain assembly on its catalytic residue. Nat Cell Biol 9, 422–427.
Reindle A, Belichenko I, Bylebyl GR, Chen XL, Gandhi N, Johnson ES (2006). Multiple domains in Siz SUMO ligases contribute to substrate selectivity. J Cell Sci 119, 4749–4757.
Sampson DA, Wang M, Matunis MJ (2001). The small ubiquitin-like modifier-1 (SUMO-1) consensus sequence mediates Ubc9 binding and is essential for SUMO-1 modification. J Biol Chem 276, 21664–21669.
Sesaki H, Jensen RE (1999). Division versus fusion: Dnm1p and Fzo1p antagonistically regulate mitochondrial shape. J Cell Biol 147, 699–706.
Shen TH, Lin H-K, Scaglioni PP, Yung TM, Pandolfi PP (2006). The mechanisms of PML-nuclear body formation. Mol Cell 24, 331–339.
Shulga N, Mosammaparast N, Wozniak R, Goldfarb DS (2000). Yeast nucleoporins involved in passive nuclear envelope permeability. J Cell Biol 149, 1027–1038.
Stehmeier P, Muller S (2009). Phospho-regulated SUMO interaction modules connect the SUMO system to CK2 signaling. Mol Cell 33, 400–409.
Sun H, Leverson JD, Hunter T (2007). Conserved function of RNF4 family proteins in eukaryotes: targeting a ubiquitin ligase to SUMOylated proteins. EMBO J 26, 4102–4112.
Szymanski EP, Kerscher O (2013). Budding yeast protein extraction and purification for the study of function, interactions, and post-translational modifications. J Vis Exp 80, e50921.
Takahashi Y, Iwase M, Strunnikov AV, Kikuchi Y (2008). Cytoplasmic sumoylation by PIAS-type Siz1-SUMO ligase. Cell Cycle 7, 1738–1744.
Takahashi Y, Kahyo T, Toh-E A, Yasuda H, Kikuchi Y (2001a). Yeast Ull1/Siz1 is a novel SUMO1/Smt3 ligase for septin components and functions as an adaptor between conjugating enzyme and substrates. J Biol Chem 276, 48973–48977.
Takahashi Y, Kikuchi Y (2005). Yeast PIAS-type Ull1/Siz1 is composed of SUMO ligase and regulatory domains. J Biol Chem 280, 35822–35828.
Takahashi Y, Toh-E A, Kikuchi Y (2001b). A novel factor required for the SUMO1/Smt3 conjugation of yeast septins. Gene 275, 223–231.
Takahashi Y, Yong-Gonzalez V, Kikuchi Y, Strunnikov A (2006). SIZ1/SIZ2 control of chromosome transmission fidelity is mediated by the sumoylation of topoisomerase II. Genetics 172, 783–794.
Tan W, Wang Z, Prelich G (2013). Physical and genetic interactions between Uls1 and the Slx5-Slx8 SUMO-targeted ubiquitin ligase. G3 (Bethesda) 3, 771–780.
Tatham MH, Geoffroy M-C, Shen L, Plechanovova A, Hattersley N, Jaffray EG, Palvimo JJ, Hay RT (2008). RNF4 is a poly-SUMO-specific E3 ubiquitin ligase required for arsenic-induced PML degradation. Nat Cell Biol 10, 538–546.
Tkach JM *et al*. (2012). Dissecting DNA damage response pathways by analysing protein localization and abundance changes during DNA replication stress. Nat Cell Biol 14, 966–976.
Ulrich HD (2008). The fast-growing business of SUMO chains. Mol Cell 32, 301–305.
Ulrich HD, Walden H (2010). Ubiquitin signalling in DNA replication and repair. Nat Rev Mol Cell Biol 11, 479–489.
Uzunova KK *et al*. (2007). Ubiquitin-dependent proteolytic control of SUMO conjugates. J Biol Chem 282, 34167–34175.
Vertegaal ACO (2010). SUMO chains: polymeric signals. Biochem Soc Trans 38, 46–49.
Wang Y, Dasso M (2009). SUMOylation and deSUMOylation at a glance. J Cell Sci 122, 4249–4252.
Wang Z, Prelich G (2009). Quality control of a transcriptional regulator by SUMO-targeted degradation. Mol Cell Biol 29, 1694–1706.
Wang Z, Jones GM, Prelich G (2006). Genetic analysis connects SLX5 and SLX8 to the SUMO pathway in *Saccharomyces cerevisiae*. Genetics 172, 1499–1509.
Wickliffe K, Williamson A, Jin L, Rape M (2009). The multiple layers of ubiquitin-dependent cell cycle control. Chem Rev 109, 1537–1548.
Xie Y, Kerscher O, Kroetz MB, McConchie HF, Sung P, Hochstrasser M (2007). The yeast Hex3.Slx8 heterodimer is a ubiquitin ligase stimulated by substrate sumoylation. J Biol Chem 282, 34176–34184.
Xie Y, Rubenstein EM, Matt T, Hochstrasser M (2010). SUMO-independent in vivo activity of a SUMO-targeted ubiquitin ligase toward a short-lived transcription factor. Genes Dev 24, 893–903.
Yao T, Ndoja A (2012). Regulation of gene expression by the ubiquitin-proteasome system. Semin Cell Dev Biol 23, 523–529.
Zhang C, Roberts TM, Yang J, Desai R, Brown GW (2006). Suppression of genomic instability by SLX5 and SLX8 in *Saccharomyces cerevisiae*. DNA Repair (Amst) 5, 336–346.
Zhao X, Blobel G (2005). A SUMO ligase is part of a nuclear multiprotein complex that affects DNA repair and chromosomal organization. Proc Natl Acad Sci USA 102, 4777–4782.